THE EFFECT OF ATHEROSCLEROSIS PROGRESSION AND EXACERBATION BY DIABETES ON FIBRINOLYSIS

THE EFFECT OF ATHEROSCLEROSIS PROGRESSION AND EXACERBATION BY DIABETES ON FIBRINOLYSIS

By LUCA DI GIUSEPPANTONIO, B.Sc.

A Thesis Submitted to the School of Graduate Studies in Partial Fulfilment of the Requirements for the Degree Master of Science

McMaster University

Master of Science (2019) McMaster University

(Department of Medical Sciences) Hamilton, Ontario

TITLE:	The effect of atherosclerosis progression and exacerbation by diabetes on fibrinolysis
AUTHOR:	Luca Di Giuseppantonio B.Sc. (Queens University of Charlotte)
SUPERVISOR:	Dr. Paul Y. Kim, Ph.D.
NUMBER OF PAGES:	xiii, 73

Lay Abstract

Atherosclerosis is a disease of the large arteries that leads to unwanted blood clot formation that restrict blood flow to the heart and the brain causing heart attack and stroke, respectively. Diabetes mellitus is a metabolic disorder characterized by elevated blood sugar levels (hyperglycemia). Hyperglycemia directly alters protein and cellular structure, and indirectly influences cardiovascular complications (*e.g.* exacerbation of atherosclerosis progression). Although fibrinolysis, the process of removing clots, has also been linked with hyperglycemia, the mechanism remains unclear. To study the effect of hyperglycemia-mediated atherosclerosis exacerbation on fibrinolysis, we used mice that are prone to atherosclerosis with and without hyperglycemia and quantified: (a) atherosclerosis (lesion size, lipids), (b) blood sugar, and (c) fibrinolysis (lysis times, coagulation/fibrinolytic factors). We found strong correlation between lesion size and lysis time but not with other fibrinolytic markers. Hyperglycemia also did not affect fibrinolysis directly. Therefore, hyperglycemia may indirectly influence fibrinolysis through atherosclerosis.

Abstract

Atherosclerosis is a chronic inflammatory disease characterized by plaque or clot build-up in the arterial vessel wall, which leads to blood vessel occlusion and consequently heart attack and stroke. Diabetes is a metabolic disorder characterized by elevated sugar (hyperglycemia), which is a known risk factor for the development and exacerbation of atherosclerosis. Recent studies identified fibrinolytic factors (*e.g.* plasminogen activator inhibitor 1 (PAI-1), thrombin-activatable fibrinolysis inhibitor (TAFI)) that are linked with worsening of atherosclerosis and diabetes. In addition, since activated TAFI (TAFIa), possesses both antifibrinolytic and anti-inflammatory properties, it is a molecule of interest within the context of atherosclerosis progression. Therefore, we hypothesize that fibrinolysis is influenced by atherosclerosis and diabetes. To test this, we used mice that are prone to developing atherosclerosis ($ApoE^{-/-}$) and hyperglycemia ($Ins2^{+/Akita}$) from which the heart and plasma samples were collected at 15- or 25-weeks of age. Overall, no differences in plasma clot lysis times were observed between male (hyperglycemic) and female (normal glycemic) $ApoE^{-/-}$:$Ins2^{+/Akita}$ mice. Quantitation of plaque volume showed a significant increase at 25-weeks compared with 15-weeks, consistent with previous reports. Closer examination revealed that in 15-week-old mice, plaque volume and PAI-1 levels displayed a trend with lysis time, but not in 25-week-old mice. The lysis times showed no difference with hyperglycemia or age. When TAFIa was inhibited, 15-week-old mice had longer lysis times compared with 25-week-old mice independent of hyperglycemia. In addition, elevation of cholesterol and triglyceride levels from hyperglycemia were only observed at 15-weeks. Total PAI-1 levels appeared to decrease

with age. TAFI zymogen levels did not change with hyperglycemia or age. Fragment 1.2 levels, which indicate coagulation activation/thrombin generation increase with age but were not correlated with hyperglycemia. Overall, hyperglycemia does not appear to impact fibrinolysis directly, but rather indirectly through atherosclerosis in ApoE$^{-/-}$:*Ins2*$^{+/Akita}$ mice.

Acknowledgements

I would like to fervently thank my supervisor Dr. Paul Kim for his continual guidance and support for the success in my graduate studies. This journey with Dr. Kim has been an invaluable experience and opportunity in academic achievement, scientific research, and more importantly personal growth. His continual support and guidance coupled with passion and expertise in science has not only driven this project but also taught me to think critically and independently in my future endeavors as a scientist. I would like to thank my committee members Dr. Peter Gross and Dr. Geoff Werstuck for their guidance and input towards the completion of the study and thank their lab members for their training and insight into this work. I would also like to acknowledge the help of our lab members Alex Friedmann, Dhulfiha Muzafar Gani, Chengliang Wu, and Samantha Marino for their continual support and guidance throughout my graduate study.

Furthermore, I would like to distinctly thank my colleague and friend, Dhulfiha, for her patience and effort in microsurgery training and support throughout the study.

Lastly, I would like to thank my family for their unconditional support as this would have not been possible without them.

Table of Contents

List of Figures:

List of Tables:

List of Abbreviations

AGE	advanced glycosylation end-product
Apo(a)	apoprotein(a)
ApoB	apolipoprotein B
ApoE	apolipoprotein E
BK	bradykinin
CPN	carboxypeptidase N
FDPs	fibrin degradation products
Fg	fibrinogen
Fn	fibrin
Fn’	plasmin-modified fibrin
Fn”	TAFIa-modified fibrin
FPR-ck	Phe-Pro-Arg-chloromethylketone
HBST	HEPES buffered saline with 0.01% Tween 80
LDL	low density lipoprotein
Lp(a)	lipoprotein(a)
LDLR	low density lipoprotein receptor
LT	lysis time
mTDP	mouse TAFI-deficient plasma
NMP	normal pooled mouse plasma
OPN	osteopontin
oxLDL	oxidatively modified LDL

PAI-1	plasminogen activator inhibitor-1
Plg	plasminogen
Pn	plasmin
PPP	platelet-poor plasma
PKC	protein kinase C
PRP	platelet-rich plasma
PV	plaque volume
RAGE	receptor for advanced glycation endproducts
ROS	reactive oxygen species
PTCI	potato tuber carboxpeptidase inhibitor
TAFI	thrombin-activatable fibrinolysis inhibitor
TAFIa	activated thrombin-activatable fibrinolysis inhibitor
TM	thrombomodulin
TNK-tPA	tenecteplase; tissue-type plasminogen activator derivative with mutations T103N and N117Q in the kringle 1 domain, and A296K, A297H, A298R, A299R in the protease domain
tPA	tissue-type plasminogen activator
uPA	urokinase-type plasminogen activator
VFK-ck	Val-Phe-Lys-chloromethylketone
VLDL	very low-density lipoprotein

Declaration of Academic Achievements

Luca Di Giuseppantonio contributed to conception and design of studies, obtained scholarship to support the studies, performed all experiments, analyzed and interpreted the data, and performed statistical analyses.

Dr. Paul Y. Kim contributed to conception and design of studies, obtained funding to support the studies, and critically reviewed and obtained results.

1 Introduction

1.1 Atherosclerosis

Atherosclerosis is typically an asymptomatic disease of the arterial system that is a major cause of cardiovascular events (Chait & Bornfeldt, 2009; Comai *et al*., 1985). It is considered to be a chronic inflammatory disease whose exact mechanism of cause is unknown but develops over the years, resulting in plaque build-up in the arterial system (Schmidt *et al*., 1994; Kanter & Bornfeldt, 2013). Rupture of these plaques result in a superimposed blood clot on the rupture, commonly known as atherothombosis. This process begins with increased arterial endothelium permeability which allows low density lipoprotein particles (LDL) to enter the intima layer of the vessel (Lusis, 2000). This usually occurs in high fluid shear stress areas such as sites of arterial bifurcations or curvatures (Lusis, 2000). These deposited LDLs are prone to oxidation, leading to vascular injury that may trigger an inflammatory response. Upon vascular injury, there is an enhancement of endothelial cell activation and cell adhesion molecule expression such as VCAM-1 and P-selectin on the surface of endothelial cells that line the lumen of the vessel wall. This cell activation may result from hyperglycemia seen in type 1 or type 2 diabetes (Schmidt *et al*., 1994). This permits monocyte and lymphocyte binding and infiltration (Cybulsky *et al*., 2001), by which the intimal monocytes differentiate into macrophages that take up LDL. These LDL-engorged macrophages become large lipid-engorged macrophages, or foam cells. These foam cells form fatty streaks in the arterial wall. Concurrently, foam cells secrete growth factors and cytokines, which amplify the inflammatory response.

Ultimately, the foam cells undergo apoptosis producing an acellular region known as the necrotic core. This necrotic core characterizes vulnerable or unstable plaques that are prone to rupture. Rupture of these plaques or lesions may result in blood clot generation superimposed on the ruptures, also known as atherothrombosis (Figure 1). Throughout lesion progression, the formation of fibrin occurs on the luminal surface, resulting in microthrombi formation. Microthrombi may be incorporated into the plaque, effectively increasing its size by transforming into fibrous tissue (Tegos *et al*., 2001; Duguid, 1946). Furthermore, thrombi formed after plaque rupture, erosion, or calcified nodule, contribute to an increase in luminal narrowing once repaired to form healed lesions (Fumiyuki, Yasuda, Noguchi, & Ishibashi-Ueda, 2016).

1.2 **Diabetes**

Diabetes is a chronic, frequently debilitating, and sometimes fatal disease where the body either cannot produce insulin or cannot properly use the insulin produced (Canadian Diabetes Association, 2017). Diabetes is classified as either type 1 (autoimmune) or type 2 (insensitivity) (Centres for Disease Control and Prevention, 2016). If left untreated, diabetes may lead to hyperglycemia, which is characterized by having fasting sugar and HbA1c levels of 7.0 mmol/L or more and 48 mmol/L (6.5% or more), respectively (Diabetes.co.uk, 2014). Chronic hyperglycemia is now recognized as the primary factor in the pathogenesis of diabetic complications (Aronson & Rayfield, 2002; Vlassara & Palace, 2002) and can damage blood cells, organs and nerves. More importantly, diabetes may accelerate cardiovascular disease, specifically atherosclerosis, as well as increases the risk

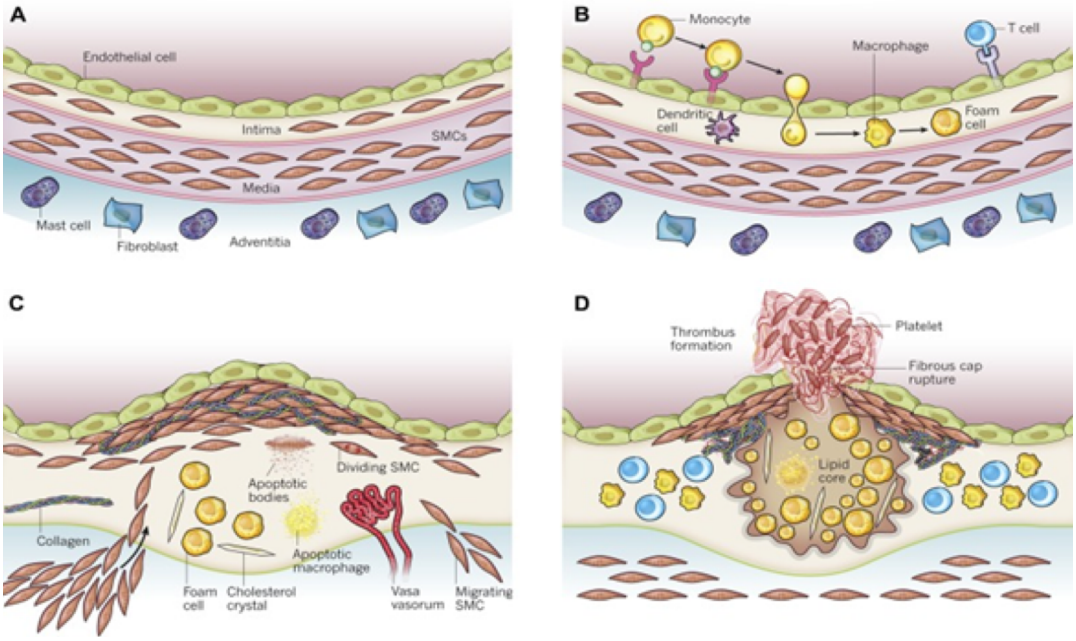

Figure 1 – Progression of atherosclerosis.
LDL infiltration into healthy vessels result in an immune response. Monocytes begin to infiltrate the vessel wall and differentiate into macrophages. These macrophages uptake LDL forming foam cells. The inflammatory response continues until the plaque ruptures and forms a thrombus. Adapted from: Lo, J., & Plutzky, J. (2012, June 1). The biology of atherosclerosis: General paradigms and distinct pathogenic mechanisms among HIV-infected patients. Journal of Infectious Diseases.

of heart disease and stroke (World Health Organization, 2013). Furthermore, 50% of people with diabetes die of cardiovascular disease (World Health Organization, 2013). In diabetes, the initiation of vascular lesions was not dependent on lipid levels but likely a consequence of hyperglycemia (Barlovic, Soro-Paavonen, & Jandeleit-Dahm, 2011); whereby, diabetes-induced hyperglycemia has been shown to accelerate atherosclerosis development independent of plasma lipid levels (Werstuck *et al*., 2006; Khan, Pichna, Bowes, & Werstuck, 2009).

1.3 **Fibrinolysis**

Fibrinolysis is the process of clot dissolution. This process is initiated *in vivo* through the release of tissue-plasminogen activator (tPA) from endothelial cells or urokinase-type plasminogen activator (uPA) from monocyte, macrophages, or the urinary epithelium (Chapin & Hajjar, 2015). tPA activates plasminogen (Plg) to plasmin (Pn), resulting in fibrin digestion. Fibrin is an insoluble protein produced when thrombin cleaves fibrinogen, a 340 kDa glycoprotein synthesized by the liver (Mosesson, 2005).

tPA-mediated Plg activation is slow and inefficient, but the presence of fibrin, however, enhances this reaction 1000-fold by acting as a template to which Plg and tPA can bind together to enhance the overall Plg activation efficiency, effectively contributing to its own degradation (Fredenburgh & Nesheim, 1992; Horrevoets, Pannekoek, & Nesheim, 1997; Hoylaerts, Rijken, Lijnen, & Collen, 1982). Pn begins to digest fibrin, which in its early stage is referred to as plasmin-modified fibrin (Fn'). The initial cleavage of fibrin generates new C-terminal lysine residues to which tPA and Plg can bind. This leads to further enhancement of Plg activation by tPA, by which Fn' has a 3-fold increased

cofactor activity compared with intact fibrin (Hoylaerts, Rijken Lijnen, & Collen, 1982; Norrman, Wallen, & Ranby, 1985). These newly generated C-terminal lysine residues act both to enhance Pn formation via binding of plasminogen as well as acting as a cofactor for Pn-mediated conversion of Glu-Plg to Lys-Plg, which is a better substrate of tPA (Declerck, 2011). To prevent bleeding that may result from this positive feedback mechanism, Pn generation is either directly inhibited by plasminogen activator inhibitors (PAIs) or α_2-antiplasmin, or indirectly by activated thrombin-activatable fibrinolysis inhibitor (TAFIa) generation (Figure 2). The activity of both uPA and tPA are regulated by PAI-1.

α_2-antiplasmin is a 464-amino acid single-chain glycoprotein that is the main physiologic inhibitor of Pn (Rijken & Lijnen, 2009). α_2-antiplasmin is a serine protease inhibitor secreted by the liver, that crosslinks to both fibrinogen and fibrin during clot formation and protects the clot from fibrinolysis (Rijken & Lijnen, 2009). In circulation, α_2-antiplasmin is both in free form and bound to Plg and fibrinogen. It down-regulates fibrinolysis in three ways. First, α_2-antiplasmin forms a stoichiometric complex with Pn where unbound Pn is inhibited more readily compared with clot-bound Pn (Carpenter & Matthew, 2008). Second, it protects the fibrin clot from degradation by Pn as it is cross-linked to both the precursor fibrinogen and fibrin by factor (F) XIIIa (Carpenter & Matthew, 2008). Third, by forming a complex with the lysine-binding sites of Plg through its C-terminus, the binding of Plg to fibrin is inhibited, resulting in down-regulation of Plg activation (Carpenter & Matthew, 2008).

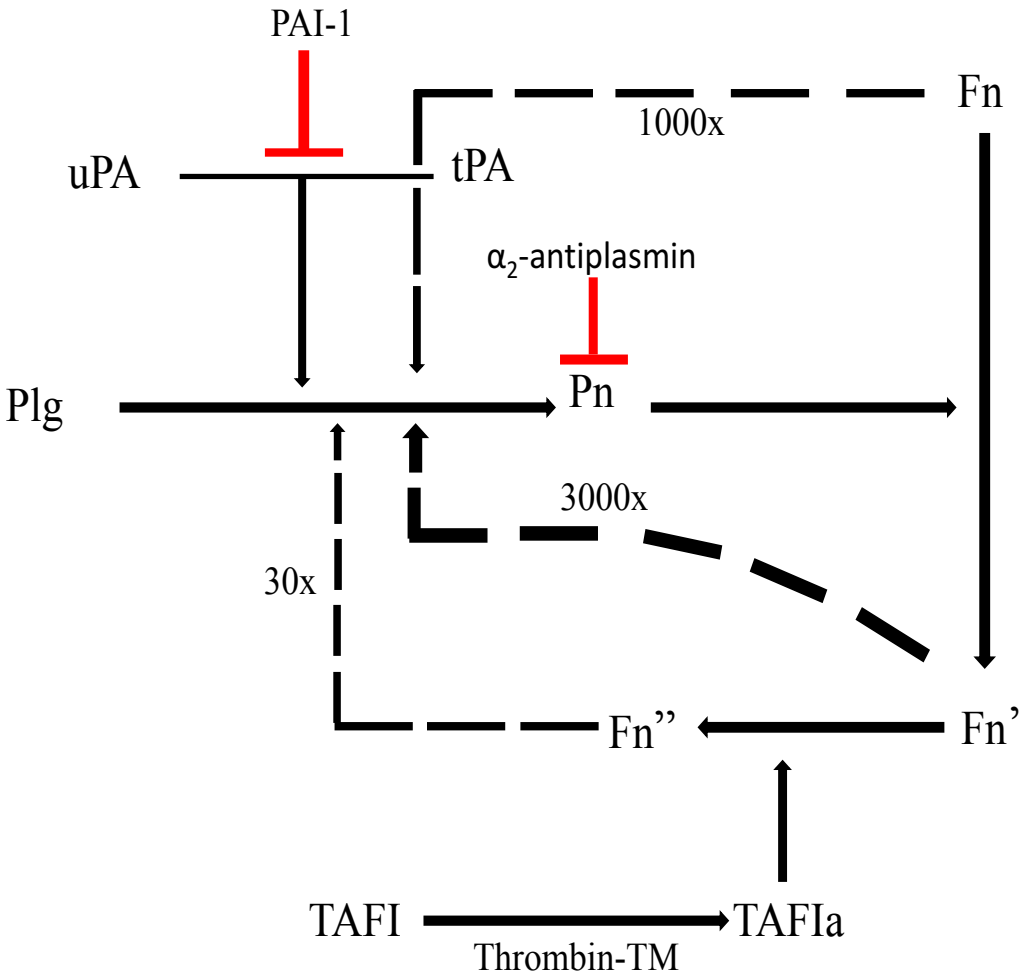

Figure 2 – Fibrinolytic pathway: Role of TAFIa in attenuating fibrinolysis.
Plasminogen (Plg) is activated to plasmin (Pn) by tissue-plasminogen activator (tPA) or urokinase plasminogen activator (uPA). This activation is upregulated 1000-fold by fibrin (Fn). Plasmin modifies fibrin, generating plasmin-modified fibrin (Fn’). Fn’ upregulates plasminogen activation to plasmin 3000-fold. Subsequently, TAFI is activated by the thrombin-thrombomodulin (TM) complex to TAFIa. TAFIa downregulates plasminogen activation to plasmin 100-fold. The activity of tPA and uPA are inhibited by plasminogen activator inhibitor 1 (PAI-1), and Pn is inhibited by α_2-antiplasmin.

1.3.1 Plasminogen activator inhibitor 1 (PAI-1)

Originating from endothelial cells, PAI-1 is a 47 kDa 379-amino acid single chain glycoprotein member of the superfamily of serpins whose antigen circulates between 6 and 80 ng/mL and acts as the chief inhibitor of tPA and uPA (Cesari, Pahor, & Incalzi, 2010; Yildiz, Kuru, Oner, & Agirbasli, 2014). PAI-1 is an important inhibitor of fibrinolysis as it directly inhibits tPA, which ultimately inhibits Pn generation. PAI-1 helps to regulate hemostasis and elevation of PAI-1 level has shown to be correlated with metabolic syndrome and their adverse outcomes (Alessi & Juhan-Vague, 2006). Therefore, PAI-1 may be a biomarker as well as a possible therapeutic target in these diseases (Yildiz *et al*., 2014).

PAI-1 is also stored in platelets, but can be secreted into the bloodstream in either an active form or complexed with tPA or vitronectin (Cesari, Pahor, & Incalzi, 2010). Vitronectin is a 70 kDa glycoprotein produced by the liver that associates with cell surfaces and can bind and stabilize PAI-1, extending its circulating lifetime, thus acting as a thrombus stabilizer by protecting fibrin from lysis (Ruggeri & Jackson, 2013; Sadler, 1997). PAI-1 mimics its substrate and forms a 1:1 complex with tPA, hindering its catalytic activity (Edelberg, Reilly, & Pizzo, 1991).

Despite its role in fibrinolysis, PAI-1 also interacts with heparin and low-density lipoprotein endocytic receptors (Cale & Lawrence, 2007). It not only serves as the physiological regulator of fibrinolysis but is associated with pathological conditions such as metabolic syndrome, obesity, cardiovascular disease, and diabetes (Cale & Lawrence, 2007; Yildiz *et al*, 2014). The ratio of tPA to PAI-1 is indicative of risk for thrombus

formation (Yildiz, *et al*., 2014), for example, PAI-1 levels are elevated in atherosclerosis which inhibit fibrinolysis and can lead to microthrombi formation or thrombus formation superimposed on the clot (Yildiz *et al*., 2014). Although present at low levels in plasma, elevation of PAI-1 has been shown in both acute and chronic diseases (Cale & Lawrence, 2007). Furthermore, PAI-1 levels rise even higher at sites of vascular injury because of its concentration in the extracellular matrix in complex with vitronectin (Cale & Lawrence, 2007). Therefore, elevation of PAI-1 may indicate worsening of preexisting conditions.

1.3.2 Thrombin-activatable fibrinolysis inhibitor (TAFI)

TAFI is a 60 kDa plasma glycoprotein (Eaton, Malloy, Tsai, Henzel, & Drayna, 1991) that is secreted by the liver and megakaryocytes as a zymogen and is activated by a distinct cleavage, forming a zinc-dependent B-like metalloprotease carboxypeptidase. Its structure consists of a 20 kDa (Phe^{1}-Arg^{92}) activation peptide and a 36 kDa (Ala^{93}-Val^{401}) catalytic domain (Marx *et al*., 2008). In circulation, TAFI exists in both the blood and platelets. In platelets, TAFI is stored within their α-granules that is released upon activation, and this accounts for <0.1% of total TAFI (Mosnier, 2003).

Regardless of its low concentration, platelets secretion of TAFI at sites of thrombus formation may help regulate fibrinolysis (Foley *et al.*, 2013). Plasma TAFI circulates at varying concentrations from 73 to 275 nM (Bajzar *et al*., 1996). Variation of plasma TAFI concentration may result from (a) TAFI variants containing Thr or Ile at position 325 which may have contrasting reactivity to commercially available ELISAs, (b) SNPs that alter mRNA stability, thus affecting TAFI gene expression, and (c) regulation of TAFI gene expression by non-genetic factors (e.g. hormones, disease, cytokines) (Foley *et al.*, 2013).

The enzymatic properties between plasma and platelet TAFI do not differ except in their glycosylation pattern, which suggests that platelet TAFI is synthesized in megakaryocytes (Foley *et al*., 2013).

TAFI is slowly activated by thrombin. When thrombin binds thrombomodulin (TM), an endothelial cell membrane receptor (Sadler, 1997), they form the thrombin-TM complex that leads to enhanced TAFI activation by 1250-fold (Rijken & Lijnen, 2009). The thrombin-TM complex exerts both an anticoagulant function through activation of protein C, as well as an anti-fibrinolytic function through activation of TAFI (Sadler, 1997). TM localization to the surface of endothelial cells proposes that the thrombin-TM complex activates TAFI atop the endothelium. However, because the fibrin clot that TAFIa cleaves extends away from the endothelium, there may be another activator of TAFI present in the fibrin-rich clot (Foley *et al.*, 2013). Pn can also activate TAFI. Pn-mediated activation of TAFI prevents premature fibrinolysis by ensuring TAFIa is generated near fibrin (Foley *et al*., 2013), although this is more speculative and requires further investigation.

There are currently no known endogenous physiological inhibitors of TAFIa. The major mechanism of TAFIa inhibition is thought to be its intrinsic thermal instability that leads to spontaneous decay and inactivation. Interestingly, the half-lives of two variants of TAFIa due to naturally occurring polymorphisms differ substantially, whereby the Ile variant displays almost double the half-life compared with the Thr variant at position 325 (Declerck, 2011). In addition, because TAFIa inactivation is spontaneous due to its thermal instability, the half-lives are also sensitive to temperature: the half-lives at 37°C are 8 minutes and 15 minutes, while at 22°C are 77 minutes and 147 minutes for the Thr and Ile

variants, respectively (Foley *et al*., 2013; Declerck, 2011). At 0°C or below, however, TAFIa is thought to be indefinitely stable. Ile^{325}-TAFIa has prolonged antifibrinolytic effect and is associated with a lessening of inflammation, which likely reflects its enhanced thermal stability compared with the Thr^{325}-TAFIa variant (Foley *et al*., 2013).

TAFIa down-regulates fibrinolysis in three ways. Firstly, it cleaves the C-terminal lysine residues from Fn', generating a TAFIa-modified fibrin (Fn"), reducing tPA and Plg binding sites for tPA-mediated Plg activation (Declerck, 2011). Secondly, because the removal of C-terminal lysine residues reduces Pn and Plg binding sites, this in turn leads to greater proportion of Pn being unbound. Since Pn is protected from inhibition by α_2-antiplasmin when bound to fibrin (Schneider *et al.*, 2004), the loss of Pn binding to fibrin effectively leads to enhanced inhibition of Pn. Lastly, the removal of C-terminal lysine residues reduces Glu-Plg conversion to Lys-Plg, which is a 20-fold better substrate for tPA-mediated activation than Glu-Plg (Horrevoets *et al.*, 1997; Hoylaerts *et al.*, 1982). The TAFIa-dependent down-regulation of fibrinolysis is a threshold-dependent mechanism: inhibition of fibrinolysis occurs indefinitely when TAFIa concentration is at or above a certain threshold value (Foley *et al*., 2013). A decline in TAFIa concentration below the threshold, however, results in the inability of TAFIa to exert its antifibrinolytic effect. The concentration of Pn dictates the critical threshold value of TAFIa, whereby higher Pn concentrations increase the TAFIa concentration needed to evoke fibrinolysis regulation. Pn concentration relies on Plg activation, which correlates with the concentration of local Plg activators and inhibitors. Factors that influence the concentration of TAFIa remaining above the threshold value include (a) TAFI concentration in plasma, (b) the degree of TAFI

activation, and (c) its stability. Only 1% of TAFI needs to be activated in order to observe half-maximal attenuation of fibrinolysis, in which a gradual rate of TAFI activation is more efficient than a brief yet substantial activation in regulating fibrinolysis (Foley *et al*., 2013).

Furthermore, recent evidence also suggests that TAFIa reduces inflammation by inactivating the anaphylatoxins C3a and C5a, thrombin-cleaved osteopontin (OPN) and bradykinin (BK), whereby, C3a is the only listed substrate that is cleaved with higher catalytic efficiency by carboxypeptidase N (CPN) (Foley *et al*., 2013). Contrastingly, TAFIa cleaves C5a, OPN and BK at a higher catalytic efficiency than CPN. Therefore, TAFI(a) may play a role in inflammatory diseases.

1.4 **Atherosclerosis and Diabetes**

Diabetes-induced hyperglycemia has been shown to accelerate atherosclerosis development independent of plasma lipid levels (Werstuck *et al*., 2006; Khan *et al.*, 2009). Atherosclerosis accounts for approximately 80% of all deaths among North American diabetic patients, where more than 75% of all hospitalization for diabetic complications are attributable to cardiovascular disease (Aronson & Rayfield, 2002). Diabetes-induced hyperglycemia induces a number of alterations in vascular tissue that potentially promote atherosclerosis. There are currently four major mechanisms that comprise pathological vascular alterations of diabetic humans and animals that can promote atherosclerosis development: 1) Non-enzymatic glycosylation of proteins and lipids, 2) oxidative stress, 3) protein kinase C (PKC) activation (Aronson & Rayfield, 2002), and 4) impaired fibrinolysis (Sobel, 2003).

1.4.1 Non-enzymatic glycosylation of proteins and lipids

Hyperglycemia often causes irreversible effects and can lead to progressive cell dysfunction; however, the exact mechanism remains unknown. An important mechanism responsible for atherosclerosis development in diabetes is the non-enzymatic glycosylation reaction in the arterial wall between glucose and proteins or lipoproteins, also known as Maillard reaction. Reversible glycosylation products form between glucose and reactive amine groups of circulating or vessel wall proteins (Aronson & Rayfield, 2002) which can continue to undergo chemical rearrangement to form advanced glycosylation end products (AGE) and can form on long-lived proteins (*e.g.* vessel wall collagen) (Flier *et al.*, 1988). This non-enzymatic modification of proteins and lipids can yield detrimental effects which may include altered platelet activation, free radical formation, and altered fibrinolysis (Singh *et al*., 2014).

Moreover, glucose concentration determines the degree of non-enzymatic glycosylation and the rate of AGE accumulation on long-lived vessel walls (Flier *et al.*, 1988). AGE formation can accelerate atherosclerosis by either a) non-receptor dependent, and b) receptor-dependent mechanisms (Aronson, & Rayfield, 2002).

1.4.1.1 Non-receptor dependent atherosclerosis acceleration by AGE formation

Protein or lipoprotein glycosylation may interfere with their normal function by altering their enzymatic activity, disrupting molecular conformation, reducing degradative capacity, and interfering with receptor recognition. For example, glycation may occur on LDL between the apolipoprotein B (ApoB) and phospholipid components, leading to functional LDL alterations and increased oxidative modification susceptibility (Aronson,

& Rayfield, 2002). Glycation of ApoB occurs on the lysine residues within the LDL receptor binding domain which are necessary for specific LDL receptor recognition. This results in LDL-receptor mediated uptake impairment, reducing glycated LDL clearance compared with native LDL (Steinbrecher, & Witztum, 1984). Evidence has shown a positive correlation with glucose levels and glycated LDL, whereby, diabetic patients have up to 4-fold higher AGE-ApoB levels (Vlassara, & Palace, 2002; Bucala *et al*., 1994). Moreover, glycated LDL are preferably recognized by macrophage scavenger receptors, possibly stimulating foam cell formation and subsequent atherosclerosis development (Aronson & Rayfield, 2002).

1.4.1.2 Receptor dependent atherosclerosis acceleration by AGE formation

AGE interaction with the cellular receptor (RAGE) play a critical role in diabetic complications (Singh *et al.*, 2014). AGE-RAGE interaction is facilitated through the binding of the V domain of RAGE, in which sustained activation mediated by receptor signaling may lead to inflammation – a mechanism proposed to be responsible for AGE-mediated pathogenicity (Singh *et al.*, 2014). The presence of RAGE has also been indicated in all atherosclerotic relevant cells such as monocyte-derived macrophages, endothelial cells, and smooth muscle cells. RAGE mediates the cellular interactions of AGEs (Schmidt *et al.,* 1994; Brett *et al.,* 1993). This AGE-RAGE interaction enhances the release of pro-inflammatory molecules, stimulates gene expression and alters cellular signaling (Barlovic *et al.*, 2011). Moreover, the AGE-RAGE interaction can cause a variety of key post-receptor events leading to the development of atherosclerosis, such as the activation of VCAM-1 and NF-$_K$B on endothelial cells, resulting in increased endothelial cell

permeability (Aronson & Rayfield, 2002; Wautier *et al*., 1996). Furthermore, the atherosclerotic mouse model lacking RAGE ($ApoE^{-/-}$:$RAGE^{-/-}$) has been shown to have a significantly reduced atherosclerotic plaque area compared to the atherosclerotic mouse model ($ApoE^{-/-}$) (Soro-Paavonen *et al*., 2008). Therefore, hyperglycemia induced AGE production in diabetes may increase AGE-RAGE interaction resulting in promotion and possibly acceleration of atherosclerosis.

1.4.2 Oxidative Stress

Oxidative stress is the disturbance in the balance of reactive oxygen species (ROS) and antioxidants. Imbalance between oxidants and antioxidants increase oxidative modification in the arterial wall. Atherosclerosis represents a heightened oxidative stress state, in which ROS mediate signaling pathways that underlie vascular inflammation in atherogenesis (Rezzani *et al.*, 2008). Thus, oxidative stress may be a key mediator in atherogenic alterations in the vasculature.

Hyperglycemia has been shown to enhance ROS formation through AGE-RAGE interaction, redox imbalance, and glucose autoxidation. Oxidative stress has been shown to be positively correlated with AGE accumulation. Glucose autoxidation can produce two free radicals, hydrogen peroxide and superoxide (Aronson & Rayfield, 2002).

Furthermore, increased intracellular glucose enhances the production of oxidants while reducing antioxidant defense (King & Loeken, 2004). For example, LDL can be oxidatively modified (oxLDL) by cells in the arterial wall, whereby, oxLDL has been shown to be highly atherogenic by inhibiting endothelial nitric oxide synthase, increasing platelet aggregation, and mediating inflammation. oxLDL are also readily taken up by

macrophages, increasing ICAM-1 formation and scavenger receptor expression (King & Loeken, 2004). Therefore, diabetes-mediated hyperglycemia increases oxidative stress through AGE formation, increased free glucose levels, and oxidatively modified proteins.

1.4.3 Protein Kinase C Activation

Hyperglycemia can cause metabolic consequences resulting from glucose transport into insulin dependent cells. Increased intracellular glucose can activate the protein kinase C (PKC) pathway through increased levels of diacylglycerol, a cofactor for PKC activation (Aronson & Rayfield, 2002; Fiorentino *et al.*, 2013; Lee *et al.*, 1989). Elevated PKC activation has been shown to be involved in many atherosclerotic promoting mechanisms such as increased ROS formation, PKC-dependent adhesion of monocytes to the endothelium, and PKC-induced monocyte differentiation to macrophage (Fiorentino *et al*., 2013). Therefore, hyperglycemia induced upregulation of the PKC pathway may cause a proatheroscleroic state and potentially accelerate atherosclerosis.

1.5 **Fibrinolysis, Atherosclerosis, and Diabetes**

A proposed mechanism by which diabetes accelerates atherosclerosis is through the impairment of the fibrinolytic system. Diabetes may impair fibrinolysis though elevated PAI-1 levels, decreased tPA levels, and glycation, resulting in altered fibrin clots that are resistant to lysis (Figure 3) (Pandolfi *et al.,* 2001; Collet *et al.,* 2006; Alzahrani & Ajjan, 2010). Similarly, elevated PAI-1 and decreased tPA levels are observed in atherosclerosis, culminating altered fibrin driven hypofibrinolysis. Therefore, altered fibrinolysis must be explored in each disease independently of each other.

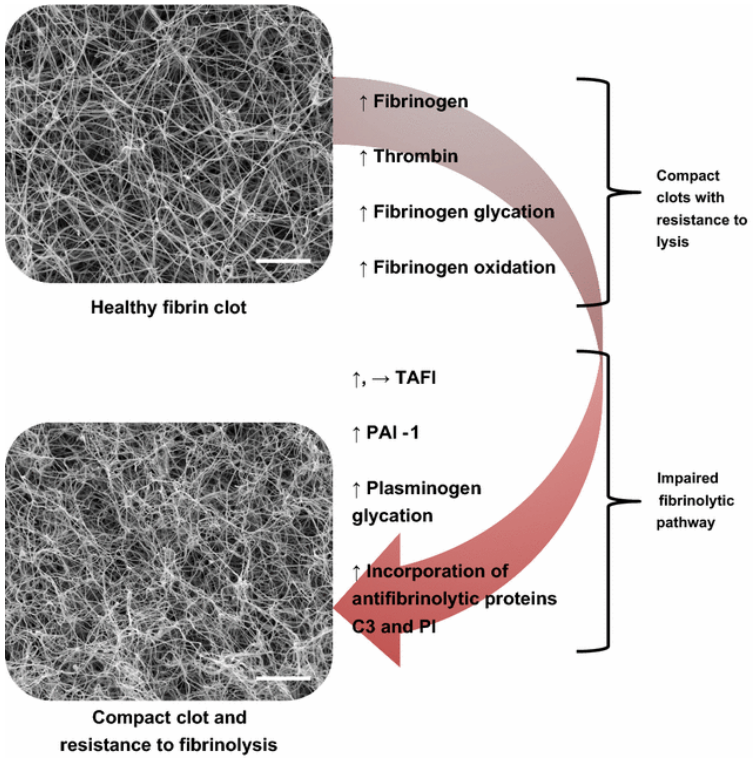

Figure 3 – Molecular mechanisms of diabetes-altered fibrinolysis.
Altered fibrin network structure and impaired fibrinolysis are the key factors in hypofibrinolysis as a result of diabetes. Altered clot structure can be attributed by increased fibrinogen, thrombin, fibrinogen glycation and fibrinogen oxidation. Elevated TAFI and PAI-1 levels, increased plasminogen glycation and incorporation of antifibrinolytic proteins into the clot impair the fibrinolytic pathway. Adapted from: Kearney, K., Tomlinson, D., Smith, K., & Ajjan, R. (2017, March 9). Hypofibrinolysis in diabetes: A therapeutic target for the reduction of cardiovascular risk. Cardiovascular Diabetology. BioMed Central Ltd.

1.5.1 Fibrinolysis and Atherosclerosis

Chronic inflammation seen in atherosclerosis could potentially enhance PAI-1 expression by the vascular endothelium. Elevated PAI-1 expression has been shown in atherosclerotic tissues and enhancement of PAI-1 levels in early stages of fibrinolysis may lessen fibrinolysis and stimulate plaque progression (Sponk, van der Voort, & ten Cate, 2004). Evidence also suggests that fibrin stiffness is an independent variable for early coronary artery disease (Collet *et al*., 2006). Elevated PAI-1 levels coupled with fibrin stiffness may contribute to fibrin deposition that can initiate and aid in plaque development. Fibrin may stimulate plaque growth by providing a scaffold to which cell proliferation and migration may occur. Impaired fibrinolysis may lead to inefficient removal of microthrombi which may be incorporated into the fibrous plaque (Collen & Juhan-Vague, 1988). Furthermore, elevated lipoprotein(a) (Lp(a)) levels are correlated with an increased risk of atherosclerosis development (Edelberg & Pizzo, 1995). Lp(a) may regulate fibrinolysis by competing with Plg activators. Lp(a) is an LDL with an apoprotein(a) subunit which is similar to Plg due to several copies of a domain homologous to the Plg kringle 4 domain, whereby, at least one Plg-like kringle 4 domain contains a lysine binding site, enabling fibrin binding (Edelberg & Pizzo, 1995; Anglés-Cano, de la Peña Díaz, & Loyau, 2001). Apo(a) is also prevented to transform into a Pn-like enzyme because of the Ser-Ile replacement at the Arg-Val Plg-activation cleavage site (Anglés-Cano, de la Peña Díaz, & Loyau, 2001). Lp(a) also competes with PAI-1, effectively prolonging Plg activation. Therefore, elevated concentrations of Lp(a) in plasma may prompt antifibrinolytic activity.

1.5.2 Fibrinolysis and Diabetes

Despite evidence that implicates fibrinolytic factors in exacerbating complications from diabetes, approximately eighty percent of diabetic deaths are attributed to thrombotic complications (Carr, 2001). The abnormal vascular endothelium observed in diabetes may play a role in increased platelet and clotting factor activation. Similarly, the fibrinolytic system is impaired in diabetes due to altered clot structure and increased antifibrinolytic proteins, such as PAI-1, exacerbating pre-existing coronary artery disease (Sobel, 2003). For example, an 18-year study observed that HbA_{1C} is positively correlated with PAI-1 levels and negatively correlated with tPA levels, demonstrating that glycaemia may modulate fibrinolysis (Alzahrani & Ajjan, 2010). Uncontrolled glycaemia can cause fibrinogen glycation, possibly contributing to altered fibrin structure (Sobel, 2003). Although no differences in fibrinogen concentration have been reported between diabetic and non-diabetic subjects, fibrinogen glycation may impair fibrinolysis by increasing fibrin permeability (Mosesson, 2005).

Moreover, compact clots with reduced pore size, increased fibre thickness, number, and branch points have been reported with chronic hyperglycemia – indicating that a post-translational modification of fibrinogen may be responsible for altered clot structure (Alzahrani & Ajjan, 2010; Jörneskog *et al*., 1996). Mechanistically, elevated glucose and oxidation observed in diabetes can increase the likelihood of post-translational modifications to fibrinolytic proteins, resulting in altered clots that are resistant to lysis (Alzahrani & Ajjan, 2010), in which prolonged clot lysis times have been observed in diabetic patients (Alzahrani & Ajjan, 2010).

Elevated plasma fibrinogen levels can increase fibre number, branch points and fibrin clot content, modulating its resistance to fibrinolysis, which highlights the relationship between altered fibrin networks and thrombosis risk (Kearney, Tomlinson, Smith, & Ajjan, 2017). Increased glycation due to hyperglycemia may result in glycation of the lysine residues on fibrinogen which may lead to more densely packed clots and reduced tPA and Plg binding sites, effectively impairing Pn-mediated clot lysis (Kearney *et al*., 2017). Moreover, ROS have the ability to covalently modify fibrinogen. Fibrinogen is highly susceptible to ROS attack, altering its spatial structure and function of the fibrin network (Rosenfeld *et al*., 2016).

Elevation of anti-fibrinolytic proteins and their incorporation into clots as observed in diabetes may contribute to a hypofibrinolytic state. The proinflammatory protein, C3, has been shown to increase clot resistance to lysis by crosslinking and binding to fibrin, however its involvement in compromising clot lysis is not entirely clear (Kearney *et al*., 2017). One study, however, demonstrated that C3 binds to Plg via lysine residues (Barthel, Schindler, Zipfel, 2012), which may interfere with tPA binding sites (Kearney *et al*., 2017). Analogously, evidence has shown an association of prolonged clot lysis time and C3 concentrations (Kearney *et al*., 2017). Furthermore, the association of TAFI levels and diabetes conceivably contribute to a hypofibrinolysis state and increased cardiovascular disease (Kearney *et al*., 2017).

Correspondingly, it has been observed in type-1 diabetic plasma that Plg conversion to Pn is reduced and generated Pn has modified activity, resulting in altered fibrinolysis

(Kearney *et al*., 2017). When plasma glucose levels are controlled, however, Plg activation and subsequent Pn activity are partially restored (Kearney *et al*., 2017).

Therefore, altered fibrinolysis in atherosclerosis and impaired fibrinolysis and hypercoagulability in diabetes creates a severely altered hemostatic system, ultimately up-regulating clot generation and down-regulating clot dissolution, which may play a role in the pathogenesis of atherosclerosis.

1.5.3 TAFI/TAFIa, Atherosclerosis, and Diabetes

TAFI, a key regulator of fibrinolysis, has shown to be positively correlated with plasma glucose levels (Alzahrani & Ajjan, 2010). However, both the role and plasma levels of TAFI or TAFIa in atherosclerosis remain unknown. Elevated PAI-1 levels, decreased tPA levels, impaired clot structure, and post-translational modifications to fibrinolytic proteins make it logical to investigate the role of TAFI or TAFIa in diabetes-mediated atherosclerosis. Additionally, the role of TAFIa in inflammation make it a plausible protein of interest in the hypofibrinolytic state in diabetes-mediated atherosclerosis progression.

1.6 **Mouse Models**

Mice typically do not readily develop atherosclerosis, even when given a high-fat diet (Zadelaar *et al*., 2002). Therefore, to investigate atherosclerosis and its progression in mice, a model deficient in apolipoprotein E ($ApoE^{-/-}$) were developed (Zhang *et al.*, 1992). $ApoE^{-/-}$ mice are homozygous for the knockout of ApoE and spontaneously develop plaques when fed a normal diet as opposed to a high cholesterol diet in $LDLR^{-/-}$ mice (Ma *et al*., 2012). ApoE is a ligand for lipoprotein receptors that mediates recognition and clearance of very low-density lipoproteins (VLDL) and chylomicrons by the liver. Therefore,

compromising ApoE activity results in inefficient clearance of lipoprotein, leading to dyslipoproteinemia. These mice develop severe hypercholesterolemia and spontaneously develop atherosclerotic plaques in the aorta (Pendse, Arbones-Mainar, Johnson, Altenburg, & Maeda, 2011). The atherosclerotic lesions observed in these mice are similar to those observed in humans, in that they include fatty streaks and fibrous plaques. Foam cell lesions are observed between 8 and 10 weeks-of-age with intermediate lesions at 15 weeks, and fibrous plaque and advanced lesions at 20 weeks (Nakashima, Plump, Raines, Breslow, & Ross, 1994). To study the effect of diabetes in atherosclerosis development and progression, hyperglycemia must be introduced into the atherosclerosis mouse model (Venegas-Pino *et al*., 2016). Fasting blood glucose levels vary in humans and mice, with levels between 3.8 and 5.5 mM for humans compared with ~9 mM for mice (The Jackson Laboratory Mouse Strain Datasheet, 2018). Diabetic hyperglycemia in mice is defined by a glucose level greater than 13 mM. Hyperglycemia is induced in our atherosclerosis model through the mutation of one copy of the insulin 2 gene (Venegas-Pino *et al*., 2016). A male *Ins2*$^{+/Akita}$ mouse is crossed with a female ApoE$^{-/-}$ mouse. The *Ins2*$^{+/Akita}$ mouse carries a point mutation in one allele of the insulin 2 gene, converting cysteine at position 96 to tyrosine (Venegas-Pino *et al*., 2016). This disrupts a disulfide bond between the insulin A and B chains, resulting in accumulation of an improperly processed proinsulin polypeptide causing endoplasmic reticulum stress-induced β-cell dysfunction (Venegas-Pino *et al*., 2016). Genetically inducing diabetes in our atherosclerosis model eliminates any potential effects that accompany drug induced hyperglycemia (Graham *et al.*, 2011). Therefore, crossing a male *Ins2*$^{+/Akita}$ mouse with a female ApoE$^{-/-}$ will effectively generate an

atherosclerotic mouse model that develops hyperglycemia (ApoE$^{-/-}$:*Ins2*$^{+/Akita}$) (Venegas-Pino *et al.,* 2016). Male ApoE$^{-/-}$:*Ins2*$^{+/Akita}$ develop chronic hyperglycemia while females are transient between 5 and 10 weeks, after which glucose levels normalize (Graham *et al.*, 2011). These mice also develop hypoinsulinemia, polydipsia, and polyuria by 4 weeks of age (Katsuda, Ohta, Shinohara, Bin, & Yamada, 2013).

1.7 **Hypothesis and aims**

Hypothesis: Hyperglycemia leads to attenuation of fibrinolysis that further accelerates atherosclerosis in a TAFIa-dependent manner.

Specific Aims:

1) Determine the effect of TAFIa on plasma clot lysis time (LT) in plasma samples collected from male and female 15- and 25-week-old ApoE$^{-/-}$:*Ins2*$^{+/Akita}$ mice.
2) Measure TAFI and PAI-1 levels in plasma samples from ApoE$^{-/-}$:*Ins2*$^{+/Akita}$ mice.
3) Quantify atherosclerosis progression by measuring the plaque volume in the aorta, and collecting the blood to measure cholesterol, lipoprotein, and blood glucose.
4) Determine degree of chronic coagulation in these mice by measuring their fragment 1.2 (F1.2) levels from isolated plasma.

2 Materials and Methods

2.1 Materials

Thrombin was obtained from the Enzyme Research Laboratories (South Bend, IN, USA). Phe-Pro-Arg-chloromethylketone (FPR-ck) and Val-Phe-Lys-chloromethylketone (VFK-ck) were obtained from EMD Millipore Corporation (Billerica, MA, USA). A recombinant tPA with six selective point mutations (threonine 103 with asparagine, asparagine 117 to glutamine, and a tetra alanine substitution at amino acids 296-299 to lysine, histidine, and two arginines, respectively; Tenecteplase (TNK-tPA) was a generous gift from Dr. Jeffrey Weitz (McMaster University, Hamilton, ON, Canada). Potato tuber carboxypeptidase inhibitor (PTCI), a TAFIa inhibitor, was obtained from Sigma (St. Louis, Missouri, USA). TAFI-deficient mouse plasma (mTDP) was prepared by pooling plasma obtained from 8 $TAFI^{-/-}$ mice. Experiments were pre-approved by the McMaster University Animal Research Ethics Board (AUP 18-02-09). Mice were housed in micro-isolator cages with controlled temperature and humidity on a constant 12h light/12h dark cycle and given access to regular chow and water *ad libitum*. Normal mouse plasma (NMP) was prepared by combining the plasma of 10 C57BL/6J wild-type (WT) mice. ELISA kit used to measure murine TAFI zymogen levels (mAb RT36A3F5, mAb RT30D8G6-HRP, and murine TAFI standards) was a generous gift from Dr. Paul Declerck (Katholieke Universiteit, Leuven Belgium). ELISA kit used to measure murine PAI-1 levels was obtained from Molecular Innovations (Novi, Michigan, USA). Reagents used to measure triglyceride and cholesterol levels in murine plasma was a generous gift from Dr. Geoff Werstuck (McMaster University, Hamilton, ON, Canada). ELISA kit used to measure murine F1.2 levels was

obtained from BioMatik (Cambridge, ON, Canada).

2.2 **Blood collection using carotid cannulation and plasma isolation**

Mice were fasted for 6 hours and their blood glucose level was measured using a glucometer and blood taken from the saphenous vein. Blood was collected from 15- and 25-week-old male and female ApoE$^{-/-}$:*Ins2*$^{+/Akita}$ mice (n=5) as previously described (Ni, Peleg, & Gross, 2012) with modifications (Figure 4). Mice were anesthetized for the duration of the procedure with 3% isoflurane. Once anesthetized, an incision was made with scissors to the neck of the mouse, exposing two lymph glands, the trachea, and the parotid and sub-lingual gland. The carotid artery was isolated and a surgical carotid clamp was placed at the proximal end of the vessel to halt the blood flow (Figure 4B). A suture knot was made on the distal end to prevent transposed blood flow. A small incision was made on the carotid artery using a micro scissor. Cannulation tubing with a 1 mm diameter was prepared by placing over the 28-gauge insulin needle on a 1 mL syringe containing 0.1 mL of sterile 4% citrate. The tubing was then inserted into the carotid artery via the incision and the tubing was then held in place with a second suture knot (Figure 4C). The carotid clamp was released and blood is drawn into the syringe (Figure 4D). The rate at which the blood was collected into the syringe was based on the heart-pump rate by the animal in order to minimize shear forces that the blood may be subjected to during collection. Citrated blood was carefully transferred into an Eppendorf tube and placed on ice immediately. This is crucial due to the intrinsic thermal instability of mouse TAFIa. The remainder of the blood was then used to isolate plasma. This was achieved via two centrifugation steps. Citrated blood (typically ~800

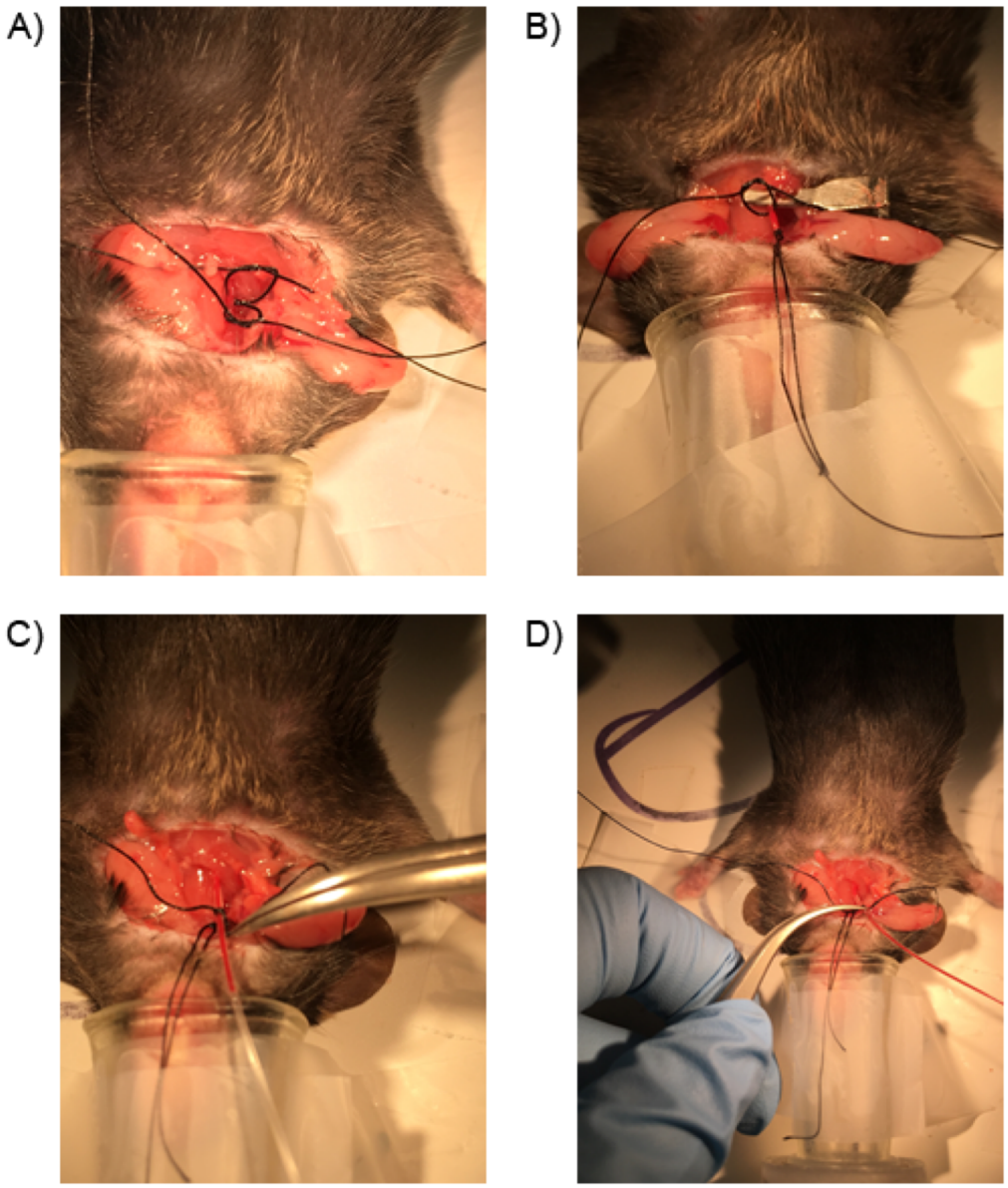

Figure 4 - Cannulation of the carotid artery.
A) Positioning and isolation of carotid artery: two loose suture knots on the carotid artery to prevent distal backflow and secure the artery in place. B) clamping of the carotid artery via the artery clamp, permitting a clean area for the incision to be made. C) Cannula inside the artery and held secure in place by the suture thread knot. Artery clip is released to allow blood to flow inside the cannula. D) drawing of blood from the artery into the cannula leading to a syringe with sterile citrate (not shown).

µL) was divided equally into two Eppendorf tubes to which pre-chilled PIPES buffer (2.5 mM Pipes, 137 mM NaCl, 4mM KCl, 0.1% glucose, pH 7.4) was added to achieve a 1:1.5 dilution (typically 200 µL), and blood was placed on ice. Once gently mixed by inversion, diluted blood was centrifuged at 200 × g for 20 minutes at 4°C. The supernatant was collected, which represents the platelet-rich plasma (PRP). PRP was then centrifuged at 3000 × g for 20 minutes at 4°C, where the supernatant was collected carefully without disrupting the pellet to achieve platelet-poor plasma (PPP) and immediately placed on ice. From the isolated PPP, 50 µL was removed and added serine protease inhibitors FPR-ck and VFK-ck to inhibit thrombin/tPA and plasmin activity, respectively, for measuring TAFIa levels in plasma (Foley *et al*., 2013). The remaining PPP was either used immediately or stored at -80°C for future use.

2.3 **Clot lysis assay**

2.3.1 Clot lysis in mouse plasma

To measure the LT of mouse plasma clots, a turbidity-based clot lysis assay was used, as previously described (Kim, Steward, Lipson, & Nesheim, 2007). Prior to use, 96-well clear bottom microtiter plates were pre-treated with HBS (20 mM HEPES, 150 mM NaCl, pH 7.4) with 1% Tween 80 and rinsed thoroughly to prevent non-specific adsorption of proteins. Clots were generated in mouse plasma with human thrombin (10 nM). Because human tPA is inefficient at activating the mouse fibrinolytic system (Matsuo, Lijnen, Ueshima, Kojima, & Smyth, 2007), we used TNK-tPA, a mutant variant of tPA. Moreover, we modified this assay by conducting clot lysis at 25°C instead of 37°C to compensate for murine TAFIa instability, which has an approximate half-life of 2.8 minutes (Hillmayer *et*

al., 2008a). Each reaction was conducted in duplicates in the absence or presence of PTCI (10 μM). Reactions were monitored by measuring the absorbance reading at 400 nm at 1 minute intervals at 25°C for 8 hours using SpectraMax M2 microplate reader (Molecular Devices, CA). LT was defined as the time required to reach the half-maximal OD change during clot degradation from the moment clot formation is initiated.

2.3.2 TNK-tPA optimization in normal mouse plasma

To identify the appropriate TNK-tPA concentration to be used, clots were formed using thrombin (10 nM) and lysis was initiated with TNK-tPA at final concentrations ranging from 0 and 200 nM. Additionally, 2 μL of $CaCl_2$ (15 mM) was added into the well prior to the addition of NMP (1:3 dilution) to prevent premature clot lysis. Reactions were conducted at 25°C and 37°C, and monitored by absorbance reading at 400 nm at 1 minute intervals for 8 hours. LTs were taken as the time required to reach half-maximal turbidity change.

2.3.3 Lysis in fresh mouse plasma using optimized TNK-tPA concentration

Attenuation of clot LTs were then investigated after determining the optimal TNK-tPA concentration in mouse plasma. To investigate this, 2 μL of $CaCl_2$ (15 mM final), 5 μL of thrombin (10 nM final), and 5 μL of TNK-tPA (20 nM final) were placed independently within the reaction well. The reaction was initiated with the addition of an 88 μL mixture containing 49.5 μL of fresh isolated mouse plasma (33 μL of mouse plasma and 16.5 μL of PIPES buffer) and 38.5 μL of Hepes Buffered Saline with 0.01% Tween 80 (HBST), resulting in a 1:3 dilution of plasma in a final reaction volume of 100 μL. The reactions

were conducted at 25°C and monitored by absorbance reading at 400 nm at 1 minute intervals. LTs were determined as described above. These experiments were conducted together with a lysis experiment initiated with NMP, acting as an internal control for variability among experiments. To determine the LTs without TAFIa-mediated clot lysis attenuation in these mice plasma samples, the lysis experiments were repeated in the presence of a TAFIa inhibitor, PTCI (10 μM), and the LT was determined. Because the LTs were much lower in the presence of PTCI, TNK-tPA concentration was halved (10 nM). To infer direct TAFIa impact on fibrinolysis, TAFIa potential on LT attenuation (ΔLT) was calculated by subtracting the LT observed with PTCI from the LT observed without PTCI.

2.4 **Lipid Quantification**

To further understand the pathophysiology of diabetes-accelerated atherosclerosis, cholesterol and triglyceride levels were quantified with Infinity reagents (Venegas-Pino *et al*., 2016). Quantification was determined *in vitro* using a chromogenic assay in a 96-well plate and compared to a standard curve generated by serially diluting cholesterol or triglyceride standard reagents with deionized water. The reactions were initiated by a proprietary reagent, and after gently mixing, their absorbance at 500 nm and 660 nm was measured.

This colormetric assay was performed in a spectrophotometer following cholesterol or triglyceride reagent addition. Absorbance was adjusted to 500 nm and 660 nm and intensities calculated were converted to concentrations with respect to the standard curve.

2.5 **Histology**

2.5.1 Harvesting and sectioning

All mice were fed a normal chow diet and harvested at 15- and 25- weeks-of-age. To quantify the extent of atherosclerotic development and progression, hearts were perfused with phosphate buffered saline (PBS) after harvest, fixed in 10% formalin, processed over-night in a tissue processor, and paraffin encased (Venegas-Pino *et al.*, 2013). Hearts encased in paraffin were subsequently trimmed at 10 μm until indication of the first aortic valve leaflet was observed. Reorientation of the block allowed for observation of the second leaflet. When two out of the three leaflets were visible, sections were taken at 5 μm and fixed to slides after being placed on a hot water bath at 40°C. Collection of the sections was distributed over 10 staggered slides running left to right and top to bottom (Venegas-Pino *et al.*, 2013). Sections were taken until there were no observable aortic valve pouches.

2.5.2 Plaque quantification

Plaque quantification were completed as previously described (Venegas-Pino *et al.*, 2013). The aortic sinus was fully sectioned after 4-8 sections taken at a thickness of 5 μm. ApoE$^{-/-}$:*Ins2*$^{+/\text{Akita}}$ sections were stained with Mason's trichrome which stains connective tissue blue, nuclei dark red/purple, and cytoplasm pink (Venegas-Pino *et al*., 2013). The first slide was stained and imaged using ImageJ software. The area of lesions present in each pouch was defined as the sum of plaques in all aortic pouches. Plaque volumes were then calculated via measurements of adjacent slides, whereby, the volume between two adjacent slides were determined by averaging the area between them and multiplying by

the section thickness (see statistical analysis). This was applied to every adjacent pair of sections from the first to tenth section in order to calculate the total volume of plaque between each pair.

2.6 **Measurement of TAFI zymogen levels in isolated plasma**

To determine if any differences in TAFI zymogen levels were present between age/genotype, TAFI levels were measured in isolated plasma samples utilizing a sandwich-type ELISA that was generously gifted by Dr. Paul Declerck (KU Leuven, Belgium) (Hillmayer *et al*., 2008b). Briefly, wells of a polystyrene microtiter plate were coated with the capture antibody against TAFI (mAb RT-36A3F5) that was diluted with PBS (0.04 M phosphate, 0.14 M NaCl, pH 7.4). After 48 hours of incubation at 4°C, the wells were emptied and PBS containing 10 g/L bovine serum albumin (BSA) were added. The plate was washed and stored at -20°C until use. Samples were then incubated in the antibody coated wells for 18 hours at 4°C. After incubation, the conjugate antibody (mAb RT 30D8G6-HRP) was added to the wells and incubated for two hours at room temperature. The wells were emptied and washed, and the substrate solution constituted with 0.1 M citrate, 0.2 M sodium phosphate buffer pH 5.0, containing 300 µg/ml *o*-phenylenediamine dihydrochloride and 0.003% hydrogen peroxide was added. Substrate solution was permitted to react for 30 minutes to one hour and stopped using 4 M sulfuric acid. The solution was then measured using absorbance at 492 nm. TAFI concentrations were then determined using specific activity specified experimentally.

2.7 Measurement of PAI-1 levels from isolated plasma

To determine if the observed LTs were correlated with circulating levels of PAI-1, PAI-1 levels were measured in isolated plasma samples utilizing a sandwich-type ELISA from Molecular Innovations (Novi, Michigan, USA). Briefly, serially diluted PAI-1 standard and murine plasma samples diluted 1:5 were added to a polystyrene microtiter plate that was pre-coated with anti-mouse PAI-1 antibody. PAI-1 standard and unknowns were incubated while shaking at 300 rpm for 30 minutes. Wells were washed and primary antibody was added to the plate for 30 minutes while shaking at 300 rpm. Wells were washed three times with wash buffer. Secondary antibody was added to the well and incubated at 300 rpm for 30 minutes and then washed three times. TMB substrate was subsequently added to the wells for 1-5 minutes and the reaction was quenched with the addition of 1N H_2SO_4 and absorbance was measured spectrophotometrically at 450 nm. The absorbance values were then plotted as a function of PAI-1 concentration to generate the standard curve. A rectangular hyperbola fit was used to determine the PAI-1 levels in the ApoE$^{-/-}$:*Ins2*$^{+/Akita}$ samples.

2.8 Measurement of F1.2 levels from isolated plasma

To determine the prothrombotic state of these mice, we measured F1.2 levels in isolated plasma samples utilizing a murine-specific sandwich-type ELISA that was a generous gift from Dr. Paul Declerck (Katholieke Universiteit, Leuven Belgium). Briefly, serially diluted fragment 1.2 standard and plasma samples diluted 1:5 were added to a polystyrene microtiter plate that was pre-coated with anti-mouse F1.2 antibody. The standard and the ApoE$^{-/-}$:*Ins2*$^{+/Akita}$ samples were incubated for 2 hours at 37°C. Liquid was

aspirated from each well and washed three times with wash buffer. Biotin-antibody was then added to each well and incubated for 1 hour at 37°C. Wells were aspirated and washed three times. HRP-Avidin was then added to every well and incubated for 1 hour at 37°C. Wells were aspirated and washed five times before the addition of the TMB substrate. Substrate was incubated for 15 to 30 minutes at 37°C. At 30 minutes, stop solution was added to each well and absorbance was measured at 450 nm and 540 nm within 5 minutes. After correction from point-zero in the standard, the A_{450} was plotted against the known amount of F1.2 and fit to a rectangular hyperbola to determine the F1.2 levels in $ApoE^{-/-}$:$Ins2^{+/Akita}$ samples.

2.9 **Statistical analysis**

Data analyses were performed using SigmaPlot (v11, SPSS Inc.). Normality of LTs was assessed using the Shapiro-Wilk test. Normally distributed data was compared using t-tests for comparisons between two groups and one- or two- way analysis of variance was used, followed by the Holm-Sidak multiple comparison test between all groups. As a means of a non-parametric test, the Kruskall-Wallis test with Dunn's post hoc test was used to analyze medians of groups. Pearson's correlation coefficient test was used to determine the degree of the relationship between two linearly related variables and to test whether there was a statistical correlation between two variables. Simple linear regression was used to determine the best-fitting straight line through data points consisting of the predicted Y score for each possible X value. Plaque volume was calculated from serial 2D images of aortic sinus cross sections by multiplying the section thickness by the average area of adjacent sections. The equation below was used to determine volume:

$$V = T\frac{(S_n + S_{n+1})}{2}$$

Where V is volume, T is section thickness, S_n and S_{n+1} are the first and next adjacent section along the aortic sinus or ascending aorta, respectively. All sections were taken at a thickness of 5 μm and converted from μm^3 to mm^3. This calculation was applied from the 1st to 10th adjacent pair of section in order to calculate the volume of plaque between the pair. Plaques did not present past the 8th section in the ApoE$^{-/-}$:*Ins2*$^{+/Akita}$ mice, so plaque volume was only measured up to 8 sections (400 μm). The sum of these sequential volumes was calculated to determine total plaque volume for each mouse and then compared between groups. P-value <0.05 was used as an indicator of significance.

3 Results

3.1 **Clot lysis in mouse plasma system**

3.1.1 TNK-tPA optimization

The TNK-tPA required to obtain the ideal clot LT was determined. When the experiments were carried out at 37°C, the LTs obtained were between 60 minutes (25 nM) and 5 minutes (200 nM) (Figure 5). At 25°C, the clots did not lyse at TNK-tPA concentrations below 10 nM, while TNK-tPA concentrations above 80 nM resulted in premature clot lysis. At concentrations between 10 and 80 nM, LT was inversely proportional to the TNK-tPA concentration (Figure 6). Based on the results, 20 nM TNK-tPA, which generated a LT of ~298.18 minutes was used for future clot lysis experiments that are performed at 25°C.

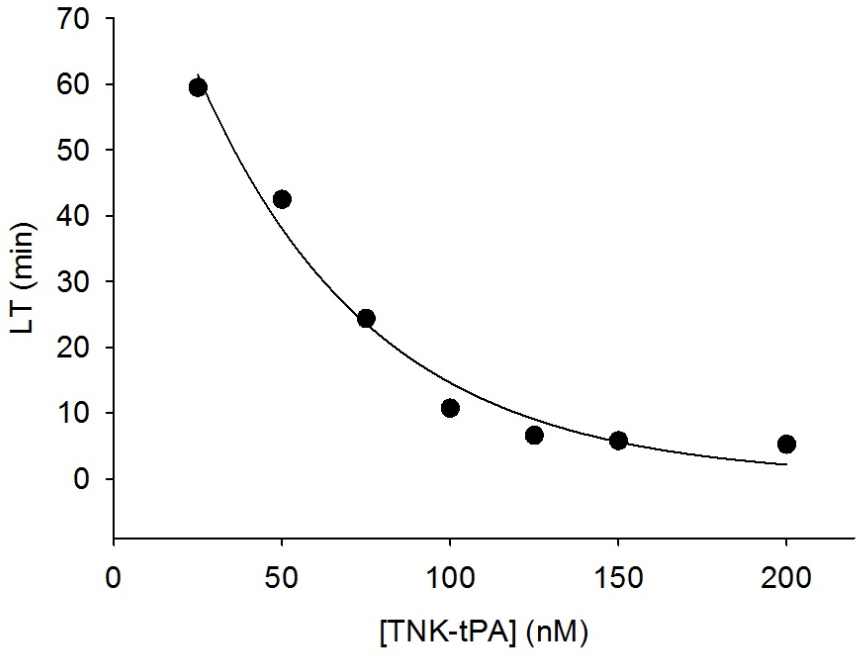

Figure 5 – LT of NMP with varying TNK-tPA concentrations at 37°C.
Plasma was clotted using thrombin and lysis was initiated with TNK-tPA at varying concentrations (0 to 200 nM) at 37°C. The reaction was monitored using turbidity at 400 nm. Time to half maximal OD change during lysis was taken as the clot LT. The LTs were then plotted with respect to TNK- tPA concentrations used. The regression line represents a line of best fit.

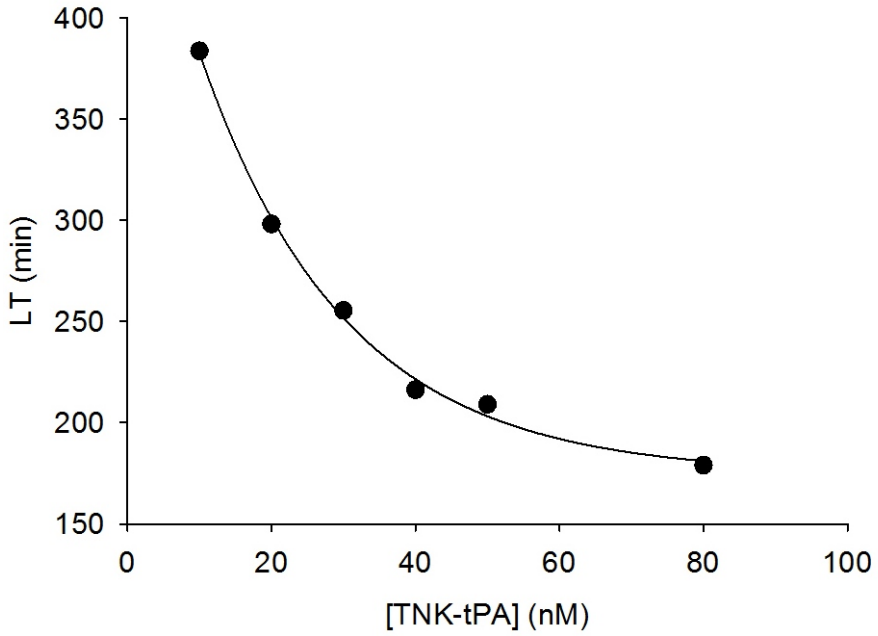

Figure 6 - LT of NMP with varying TNK-tPA concentrations at 25°C.
Plasma was clotted using thrombin and lysis was initiated with TNK-tPA at varying concentrations (0 to 100 nM) at 25°C. The reactions were monitored using turbidity at 400 nm. Time to half-maximal OD change during lysis was taken as the clot LT. The LTs were then plotted with respect to TNK-tPA concentrations used. The regression line represents a line of best fit.

3.1.2 Turbidimetric clot lysis assay using mouse plasma

All mice were catalogued and weight and fasting blood glucose levels were recorded before use. There were no differences observed in the weight of 15- and 25-week-old male and female ApoE$^{-/-}$:*Ins2*$^{+/Akita}$ mice (Table 1). Males at both 15 and 25 weeks of age were observed to have significantly greater blood glucose levels compared to their female counter parts, consistent with previously published data ($p<0.001$ and $p=0.008$, respectively) (Table 1) (Venegas-Pino *et al*., 2016). The LTs obtained using 20 nM TNK-tPA to induce fibrinolysis showed no significant differences with respect to age and sex (hyperglycemia), despite the trend of LTs being high by (a) 10-15% with hyperglycemia, and (b) 20-28% in 15-week-old mice compared with 25-week-old mice (Table 2). When the individual LT and glucose values for each mouse were considered using a two-way ANOVA, there was no apparent interaction (Figure 7).

When PTCI was added, the LTs decreased across all groups compared to reactions without PTCI. Therefore, a lower TNK-tPA concentration (10 nM) was used to determine the LTs under these conditions (Table 2). The LTs of the 15-week-old mice were significantly longer than the 25-week-old mice ($p=0.004$), independent of hyperglycemia (sex) (Figure 8).

Since LTs differ in the absence of TAFIa (*i.e.* presence of PTCI) between age groups, we postulate that TAFIa normalizes the clot LTs. Therefore, to quantify the proportion that TAFIa normalizes clot LTs for each group of mice, ΔLT was calculated and summarized (Table 2).

Age (wks)	Atherosclerotic Parameter	Male	Female	Significance
15	Weight (g)	22.82 ± 1.02	20.83 ± 2.32	
	Glucose (mM)	28.70 ± 4.94	10.88 ± 1.92	*
	Cholesterol (mM)	4.77 ± 0.36	2.35 ± 0.21	†,‡
	Triglyceride (mM)	0.21 ± 0.05	0.16 ± 0.03	†
	PV (mm^3)	0.018 ± 0.005	0.029 ± 0.027	†
25	Weight (g)	23.90 ± 1.53	22.80 ± 2.51	
	Glucose (mM)	30.48 ± 4.04	12.88 ± 2.65	*
	Cholesterol (mM)	3.86 ± 0.48	3.34 ± 0.21	
	Triglyceride (mM)	0.33 ± 0.07	0.27 ± 0.02	
	PV (mm^3)	0.124 ± 0.096	0.051 ± 0.014	

Table 1 - Atherosclerotic parameters.
Atherosclerotic parameters which include weight, fasting blood glucose levels, plasma cholesterol levels, plasma triglyceride levels, and plaque volume (PV) were measured in male and female $ApoE^{-/-}$:$Ins2^{+/Akita}$ mice at 15- and 25-weeks-of-age (n = at least 4). No differences were observed in weight when age and sex matched. Fasting glucose levels were significantly elevated in both 15- and 25-week-old males when compared to their female counter part ($p<0.001$). Plasma cholesterol levels were significantly elevated in male mice compared to female mice independent of age ($p<0.001$) and plasma cholesterol levels were significantly elevated in hyperglycemic mice when compared to normal glycemic mice ($p<0.001$). Plasma triglyceride levels were significantly elevated in 25-week-old mice compared to 15-week-old mice independent of sex ($p<0.05$). PV was significantly elevated in 25-week-mice compared to 15-week-mice independent of sex ($p<0.05$). Data are presented as a mean ± S.D. Significance between age-matched mice indicated with an asterisk (*). Significance between age groups independent of sex indicated with a single cross (†). Significance between hyperglycemic and normal glycemic groups is indicated with a double cross (‡).

Age (wks)	Hemostatic Parameter	Male	Female	Significance
15	TAFI (nM)	121.38 ± 117.64	115.39 ± 38.11	
	F1.2 (pM)	153.78 ± 39.2	134.53 ± 82.41	
	PAI-1 (ng/mL)	3.72 ± 1.04	0.922 ± 1.3	*
	LT (min)	204.31 ± 20.77	183.01 ± 17.61	
	LT with PTCI (min)	59.79 ± 3.94	61.31 ± 3.04	†
	ΔLT (min)	144.53 ± 50.3	132.70 ± 38.19	
25	TAFI (nM)	114.8 ± 56.31	108.36 ± 108.00	
	F1.2 (pM)	553.61 ± 256.45	1644.16 ± 1684.83	
	PAI-1 (ng/mL)	3.45 ± 0.79	0.960 ± 0.39	*
	LT (min)	169.64 ± 19.16	142.83 ± 22.90	
	LT with PTCI (min)	46.85 ± 4.75	44.74 ± 5.63	
	ΔLT (min)	130.6 ± 67.1	98.1 ± 52.04	

Table 2 - Hemostatic parameters.
Hemostatic parameters which include TAFI zymogen levels, F1.2 levels, PAI-1 levels, LT in the absence and presence of PTCI, and the ΔLT were measured in male and female ApoE$^{-/-}$:*Ins2*$^{+/Akita}$ mice at 15- and 25-weeks-of-age (n = at least 4). No differences were observed for TAFI zymogen levels, F1.2 levels, and LT in the absence of PTCI when age and sex matched. PAI-1 levels were significantly elevated in 15-week-old male ApoE$^{-/-}$:*Ins2*$^{+/Akita}$ compared to their female counterpart ($p<0.001$). LT in the presence of PTCI were significantly longer in 15-week-old mice compared to 25-week-old mice independent of sex ($p<0.01$). Data are presented as a mean ± S.D. Significance for age-matched mice ($p<0.001$) indicated with an asterisk (*) and significance between age groups independent of sex ($p<0.01$) indicated with a single cross (†).

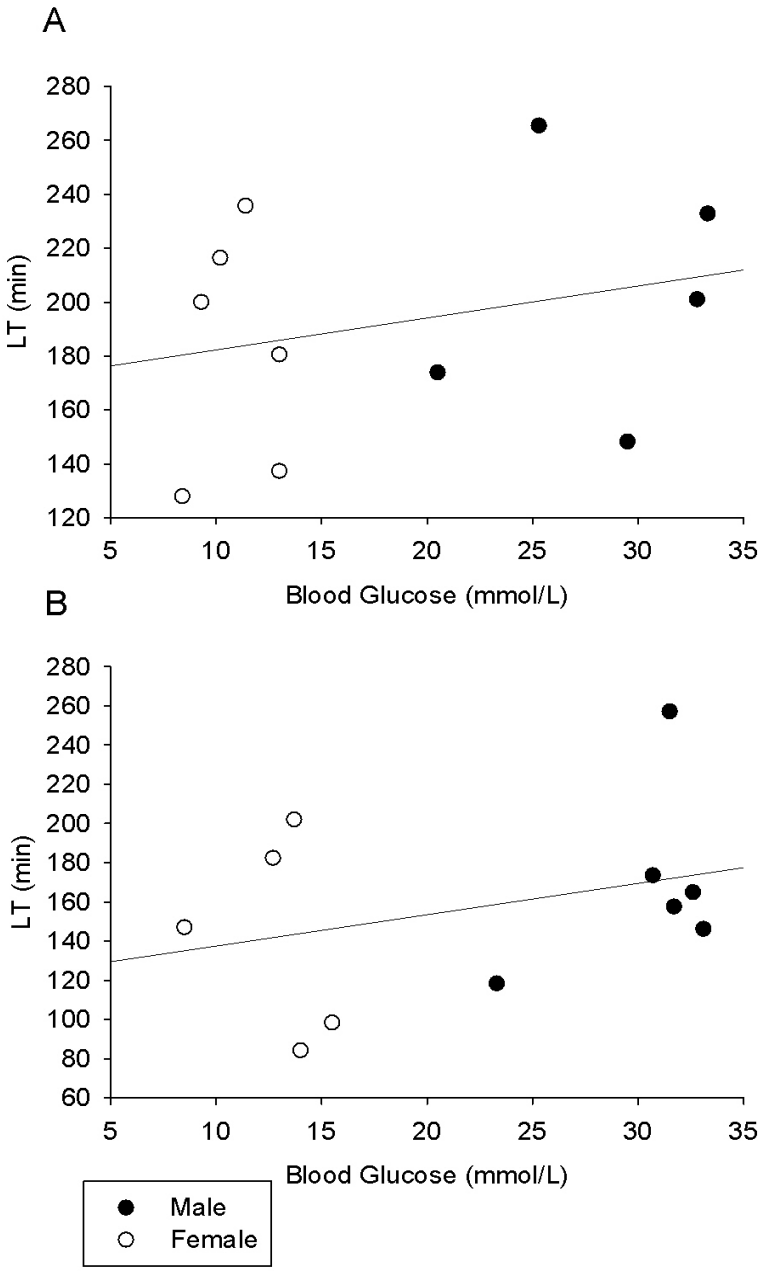

Figure 7 – The effect of blood glucose concentration on clot lysis in ApoE$^{-/-}$:*Ins2*$^{+/Akita}$ mice.

LTs in the absence of PTCI were plotted as a function of blood glucose concentration in (A) 15- and (B) 25-week-old ApoE$^{-/-}$:*Ins2*$^{+/Akita}$ mice, for both males (*closed*) and females (*open*). Using Pearson's correlation coefficient test, no correlation was observed between fasting blood glucose and LTs in the absence of PTCI. The regression line represents a line of best fit. (n = at least 5).

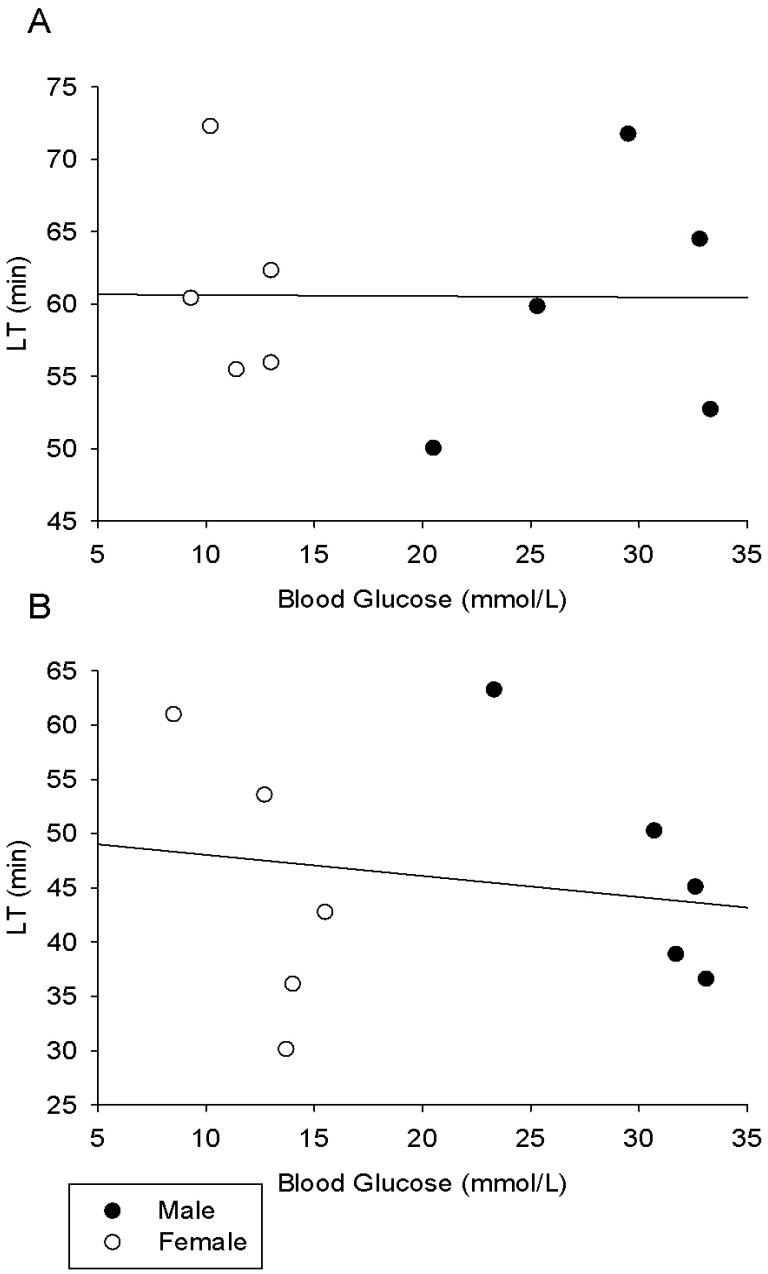

Figure 8 – The effect of blood glucose concentration on clot lysis in the presence of PTCI in ApoE$^{-/-}$:*Ins2*$^{+/Akita}$ mice.

LTs in the presence of PTCI were plotted as a function of blood glucose levels in (A) 15- and (B) 25-week-old ApoE$^{-/-}$:*Ins2*$^{+/Akita}$ mice, for both males (*closed*) and females (*open*). Using Pearson's correlation coefficient test, no correlation was observed between LTs in the presence of PTCI and fasting blood glucose levels. The regression line represents a line of best fit. (n = at least 5).

The contribution of TAFIa, indicated by ΔLT, is reduced in 25-week-old mice (10% for males and 26% for females) compared to their 15-week counterpart. Therefore, these data suggest that TAFIa may be compensating for the increased LT in an age-dependent manner, achieving normalized LTs and fibrinolysis in each category. Moreover, females have reduced ΔLT (8% for 15-weeks and 25% for 25-weeks) compared to their male counterpart, suggesting that hyperglycemia may influence LTs in a TAFIa-dependent manner.

3.2 Quantitation of plasma lipid levels

The cholesterol levels in the ApoE$^{-/-}$:*Ins2*$^{+/Akita}$ mice plasma are outlined above (Table 1). Males (hyperglycemic) showed significantly elevated plasma cholesterol levels when compared with the females (normal glycemic) ($p<0.001$). Also, 25-week-old mice showed significantly elevated plasma cholesterol levels compared with the 15-week-old mice independent of fasting blood glucose levels ($p<0.001$). While the trend is consistent with previously published data, our observed values are markedly lower: the published data list plasma cholesterol levels between 15 and 20 mM compared with our 2 and 4 mM for females, while published data for males are between 20 and 30 mM compared with our 4 to 8 mM (Venegas-Pino *et al*., 2016). Furthermore, the cholesterol levels we measured are lower than ApoE$^{-/-}$ mice fed a regular chow diet (434 mg/dL (~11.2 mM)), but coincide with C57Bl/6 mice fed a regular chow diet (86 mg/dL (~2.22 mM)) (Jawień, Nastalek, & Korbut, 2004).

Furthermore, when the plasma samples were measured for triglycerides (Table 1), 25-week-old mice had significantly elevated plasma triglyceride levels compared with their

15-week-old counterpart. Two-way ANOVA with Holm-Sidak multiple comparison test indicated that the difference observed in triglyceride levels were also independent of sex, inferring glycemic index ($p<0.01$).

3.3 TAFI zymogen measurement in mouse plasma

TAFI zymogen level in the mouse plasma samples (121 ± 117 nM) were consistent with those reported in literature (Hillmayer *et al.,* 2008a). One-way ANOVA indicate no differences with TAFI levels between age and sex groups (Table 2). When the measured LTs for each of the plasma samples were plotted against the TAFI levels, there was no observable trend between LT and TAFI levels in the absence (Figure 9) or presence (Figure 10) of TAFIa inhibitor, PTCI.

3.4 Atherosclerotic plaque quantification

The heart with the ascending aorta was sectioned and the aortic sinus was stained with Mason's trichrome to visualize cellular organization by contrasting the blue collagen of the aortic wall with the pink and red from plaques. We observe that 25-week-old mice had significantly elevated plaque volumes compared with their 15-week-old counterpart ($p=0.012$) (Table 1). To determine the correlation between elevated blood glucose and plaque volume, we plotted plaque volume as a function of blood glucose levels (Figure 11). While there was weak apparent association at 15-weeks of age (Figure 11A), largely due to the deviation with the female mice (normal glycemic), positive association was observed at 25-weeks of age (Figure 11B).

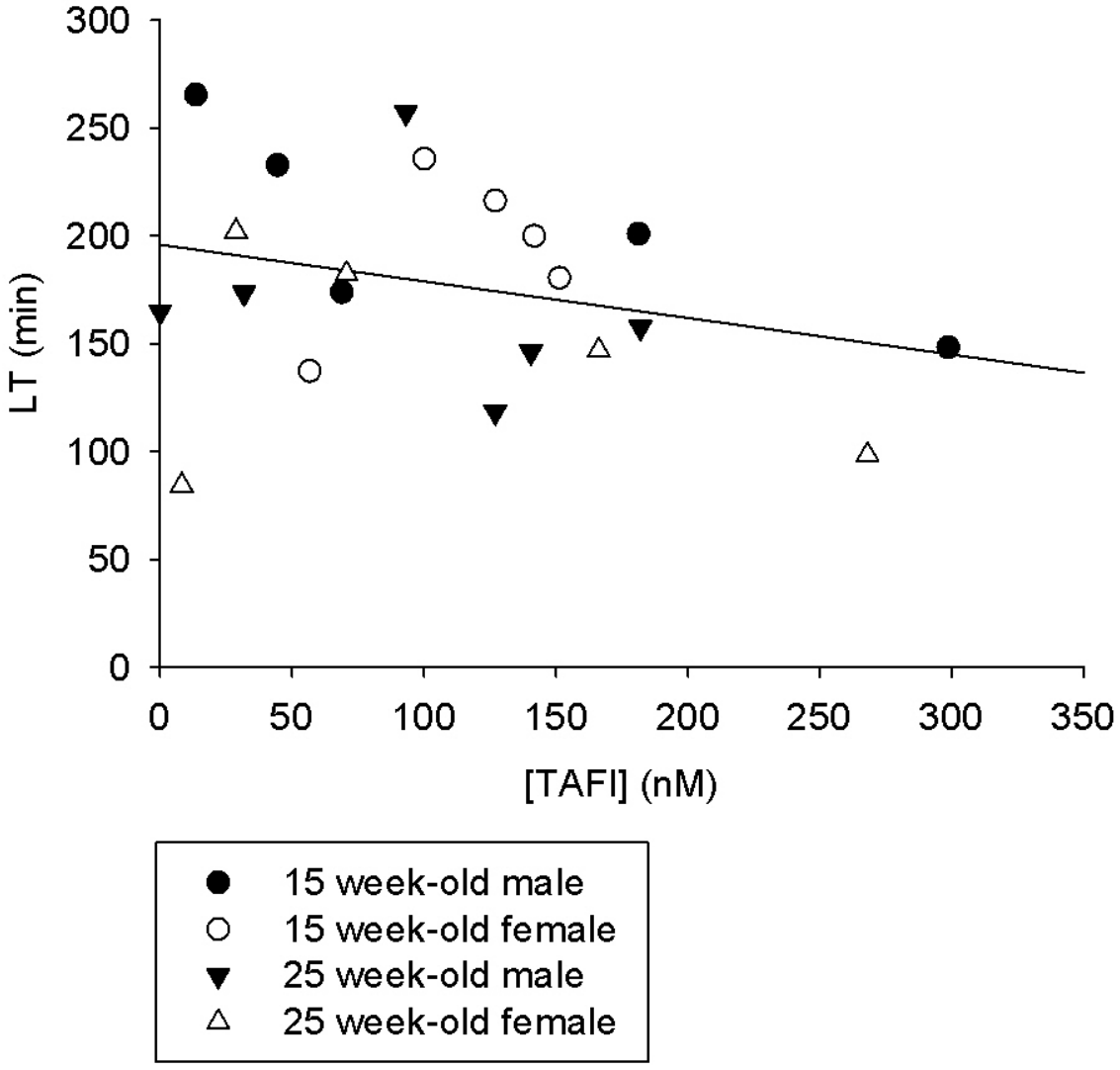

Figure 9 – The effect of TAFI concentration on clot lysis in ApoE$^{-/-}$:*Ins2*$^{+/Akita}$ mice. LT was plotted with respect to measured TAFI levels in 15- (*circle*) and 25-week-old mice ApoE$^{-/-}$:*Ins2*$^{+/Akita}$ mice, for both males (*closed*) and females (*open*). Using Pearson's correlation coefficient test, no correlation was observed between TAFI and LT. The regression line represents a line of best fit. (n = at least 5).

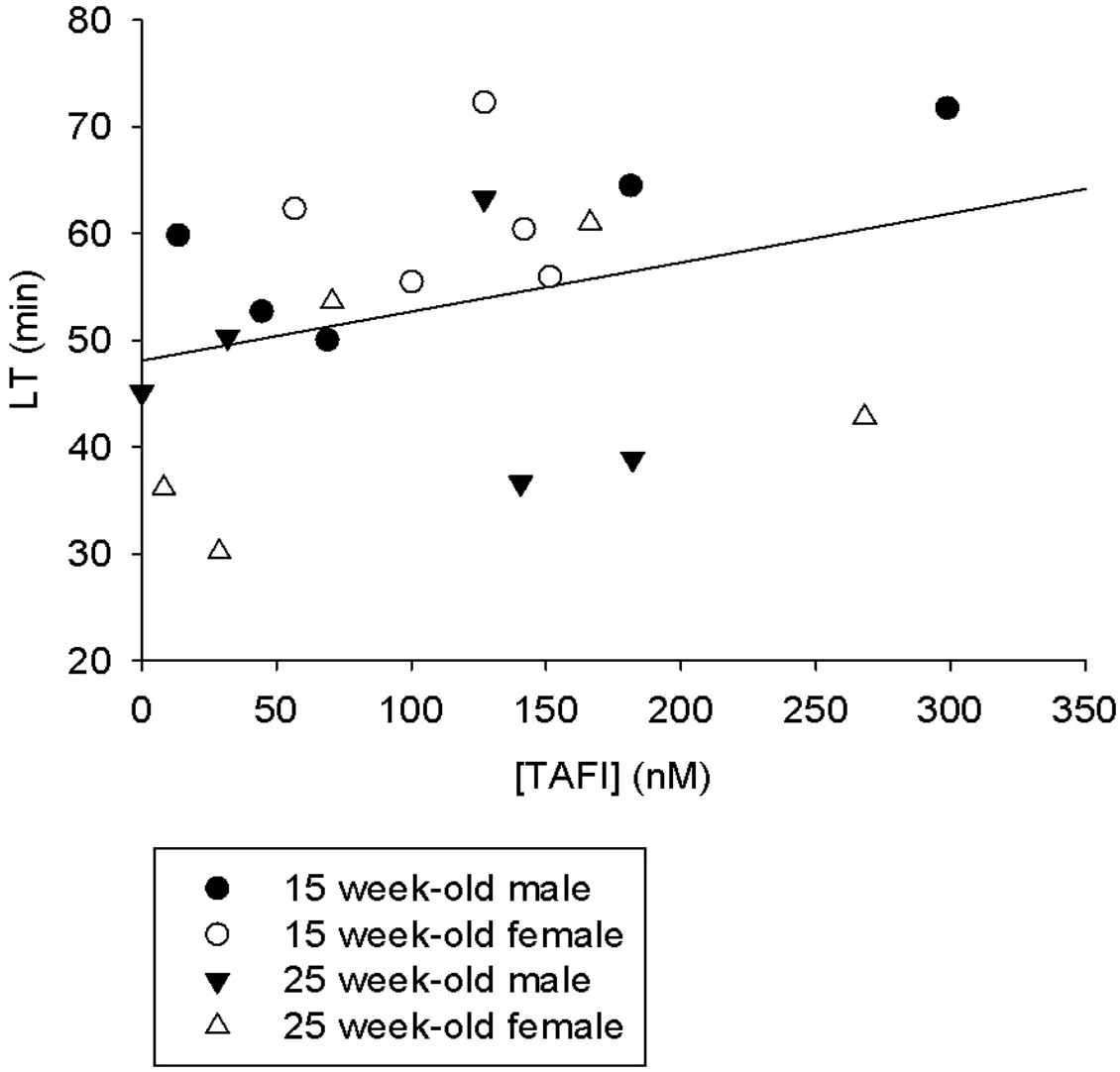

Figure 10 - The effect of TAFI concentration on clot lysis in the presence of PTCI in ApoE$^{-/-}$:*Ins2*$^{+/Akita}$ mice.

LT in the presence of PTCI was plotted with respect to measured TAFI levels in 15- (*circle*) and 25-week-old ApoE$^{-/-}$:*Ins2*$^{+/Akita}$ mice, for both males (*closed*) and females (*open*). Using Pearson's correlation coefficient test, no correlation was observed between TAFI and LTs in the presence of PTCI. The regression line represents a line of best fit. (n = at least 5).

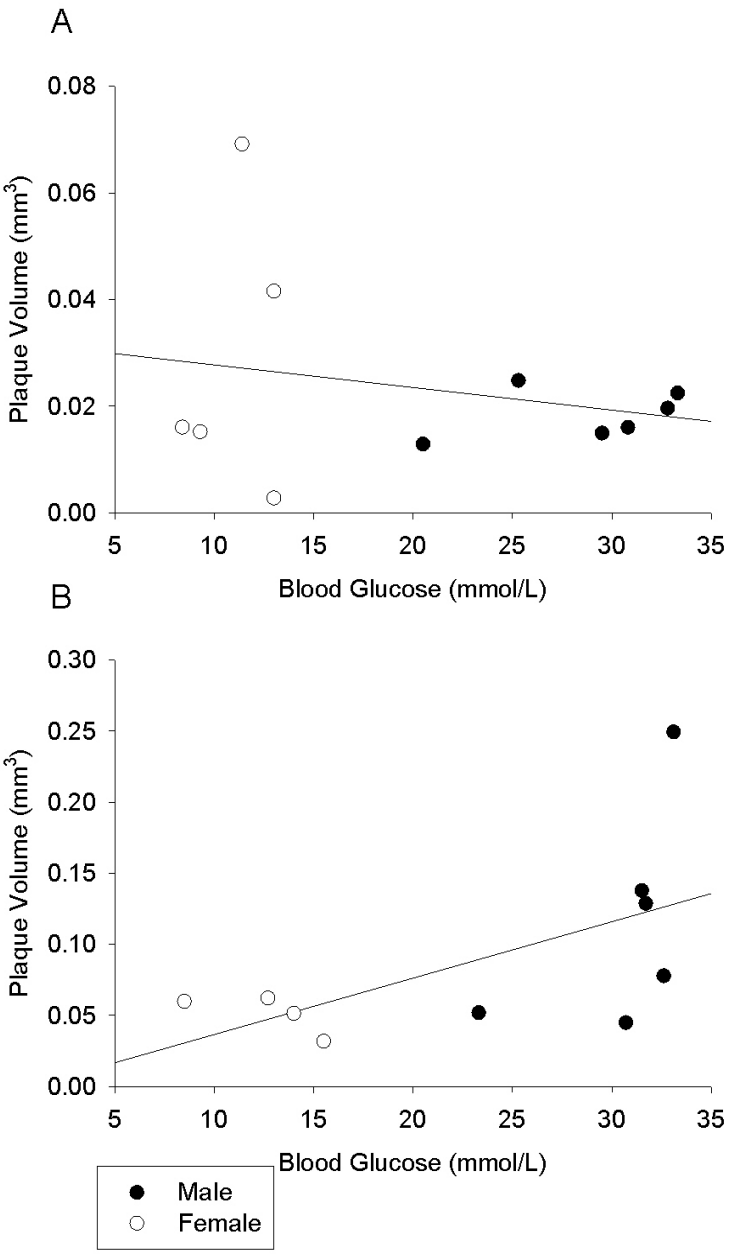

Figure 11 – Effect of blood glucose concentration on plaque volume in ApoE$^{-/-}$:*Ins2*$^{+/Akita}$ mice.

Plaque volume was plotted against fasting blood glucose levels in (A) 15-week-old and (B) 25-week-old ApoE$^{-/-}$:*Ins2*$^{+/Akita}$ mice, for both males (*closed*) and females (*open*). Using Pearson's correlation coefficient test, no correlation was observed between plaque volume and blood glucose levels. The regression line represents a line of best fit. (n = at least 4).

We then investigated the relationship between cholesterol or triglycerides, and plaque volume. The plaque volume and plasma cholesterol levels are inversely proportional at 15-weeks, while there appears to be a trend at 25-weeks (Figure 12). Similarly, plasma triglyceride levels were measured and compared with the plaque volume (Figure 13). There is no apparent trend between plaque volume and plasma triglyceride levels at 15-weeks of age, while a trend is observed at 25-weeks of age. Furthermore, when TAFI zymogen levels were compared with plaque volume, there were no apparent trends (Figure 14). We then determined whether plaque volumes are correlated with LTs (Figure 15). A trend was observed between plaque volume and LTs (*i.e.* greater inhibition of fibrinolysis with increasing plaque volume) in the 15-week mice (Figure 15A), a trend that was more prominent in females than males, while there was no apparent trend in the 25-week mice (Figure 15B).

3.5 **Measurement of F1.2 in mouse plasma**

To determine whether age or hyperglycemia (sex) leads to differences in their procoagulant state, F1.2, which are indicators of thrombin generation were measured by ELISA. The F1.2 levels ranged between 134.53 pM and 1644.16 pM with no statistical significance across age and hyperglycemia (Table 2). The F1.2 values, however, showed large discrepancies, especially in the 25-week-old mice.

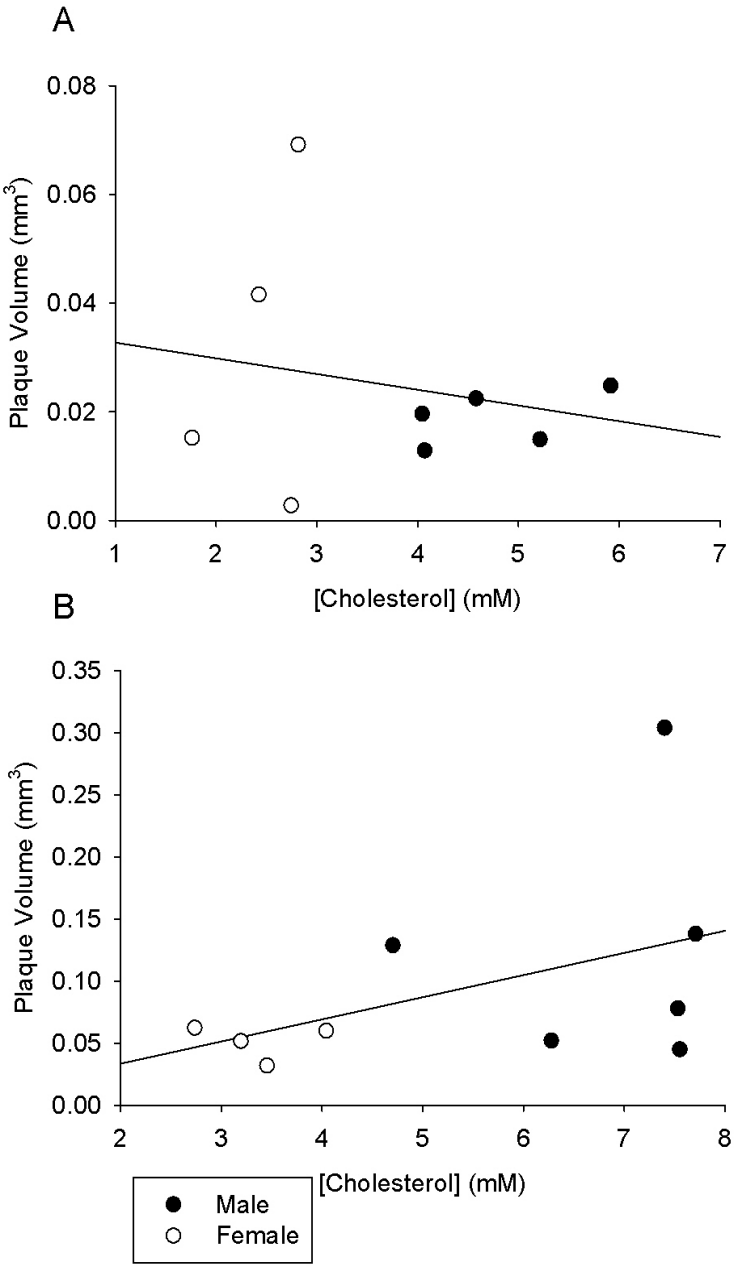

Figure 12 –Effect of plasma cholesterol concentration on plaque volume in ApoE$^{-/-}$:*Ins2*$^{+/Akita}$ mice.

Plaque volume was plotted against plasma cholesterol levels in (A) 15-week-old and (B) 25-week-old ApoE$^{-/-}$:*Ins2*$^{+/Akita}$ mice, for both males (*closed*) and females (*open*). Using Pearson's correlation coefficient test, no correlation was observed between plaque volume and plasma cholesterol levels. The regression line represents a line of best fit. (n = at least 4).

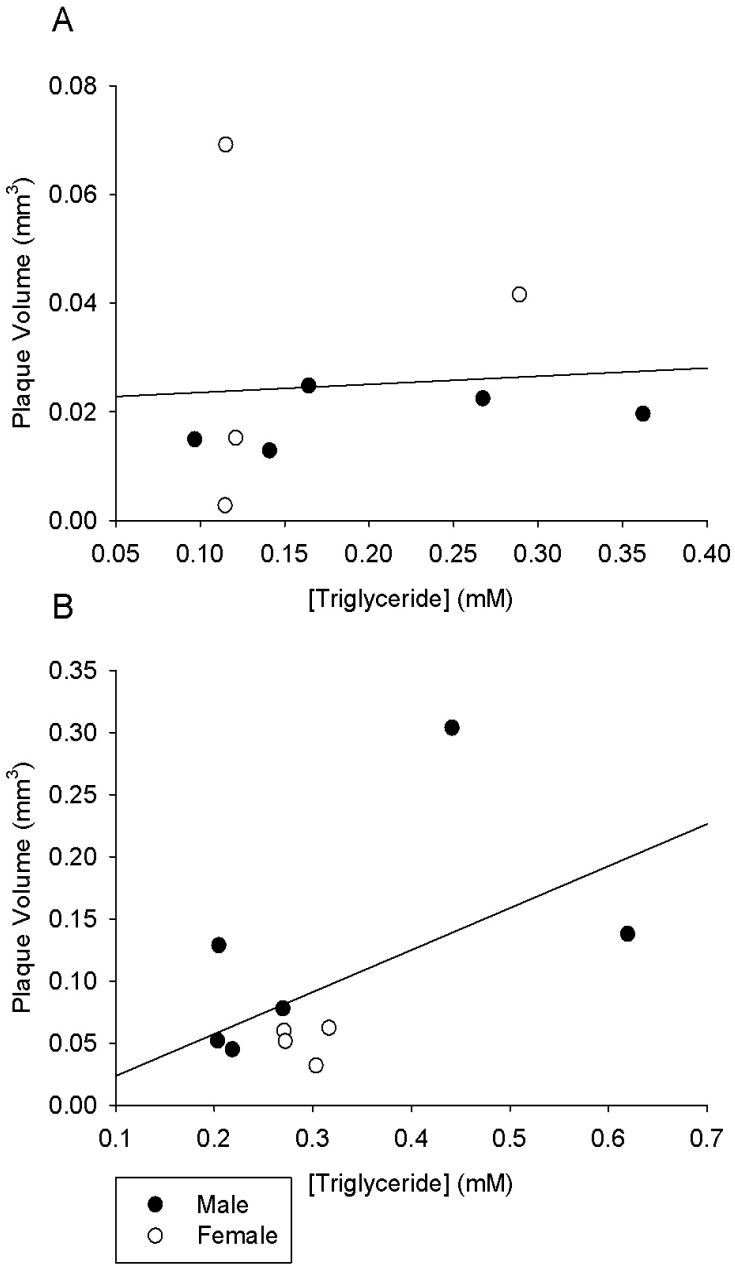

Figure 13 – Effect of plasma triglyceride concentration on plaque volume in ApoE$^{-/-}$:*Ins2*$^{+/Akita}$ mice.

Plaque volume was plotted against plasma triglyceride levels in (A) 15-week-old and (B) 25-week-old ApoE$^{-/-}$:*Ins2*$^{+/Akita}$ mice, for both males (*closed*) and females (*open*). Using Pearson's correlation coefficient test, no correlation was observed between plaque volume and plasma triglyceride levels. The regression line represents a line of best fit. (n = at least 4).

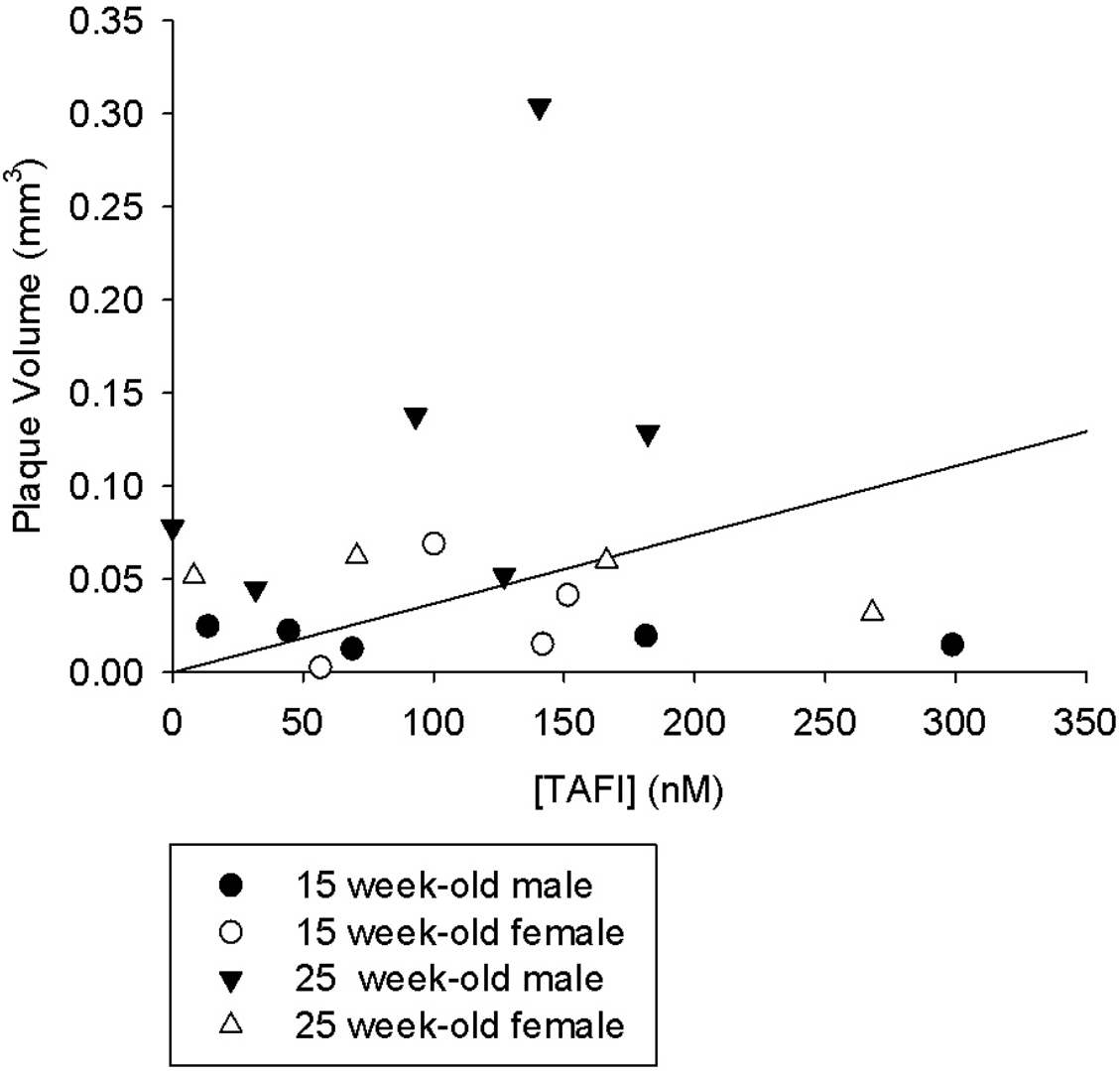

Figure 14 – Effect of plasma TAFI zymogen levels on plaque volume in ApoE$^{-/-}$:*Ins2*$^{+/Akita}$ mice.

Plaque volume was plotted against TAFI zymogen levels in 15-week-old (*circle)* and 25-week-old ApoE$^{-/-}$:*Ins2*$^{+/Akita}$ mice, for both males (*closed*) and females (*open*). Using Pearson's correlation coefficient test, no correlation was observed between plaque volume and TAFI levels. The regression line represents a line of best fit. (n = at least 4).

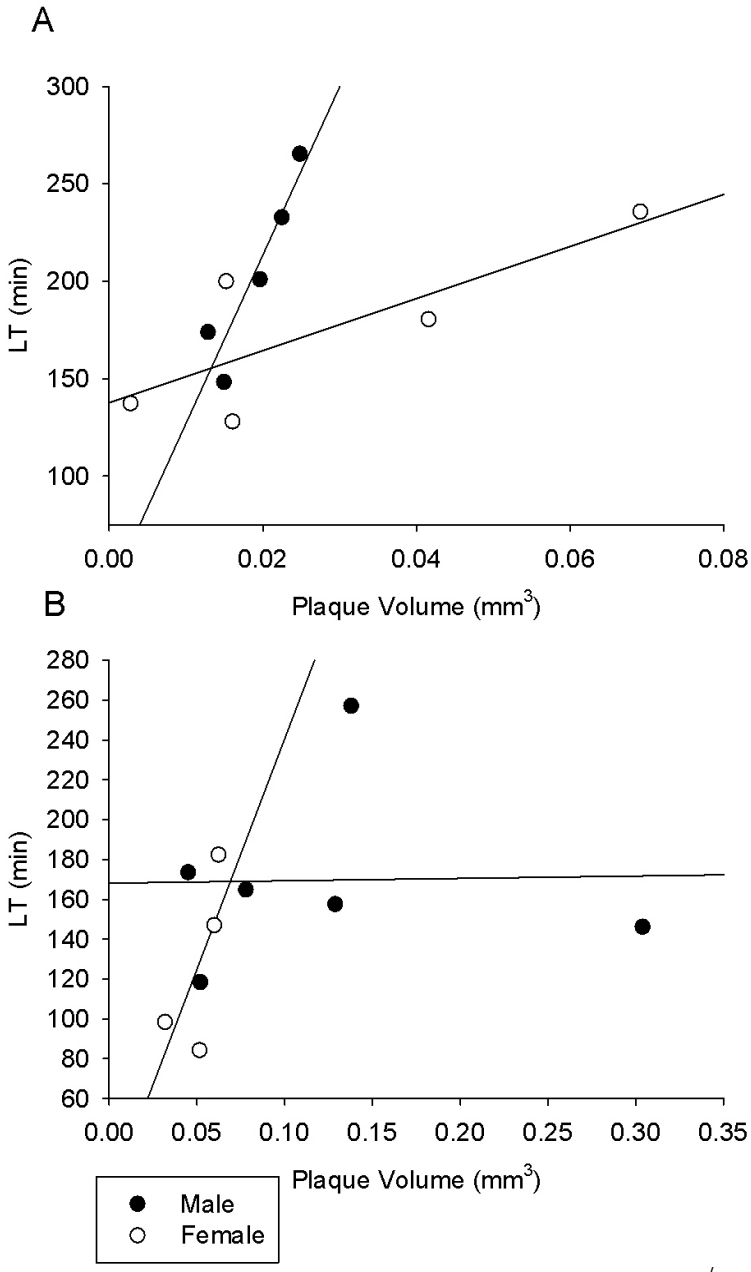

Figure 15 – Comparison of clot lysis with plaque volume in ApoE$^{-/-}$:*Ins2*$^{+/Akita}$ mice. LTs were plotted against plaque volume in (A) 15-week-old and (B) 25-week-old ApoE$^{-/-}$:*Ins2*$^{+/Akita}$ mice, for both males (*closed*) and females (*open*). Using Pearson's correlation coefficient test, no correlation was observed between plaque volume and LTs. The regression line represents a line of best fit. (n = at least 4).

3.6 **Measurement of PAI-1 in mouse plasma**

To estimate the fibrinolytic potential in plasma samples, PAI-1 levels were measured using ELISA. The PAI-1 levels ranged from 0.92 ng/mL to 5.43 ng/mL. We observe a significant difference between 15-week-old males and females ($p<0.001$), and 25-week-old males and females ($p=0.001$) (Table 2). Correlation between PAI-1 and LT (Figure 16) or plaque volume (Figure 17) was then investigated using Pearson's correlation coefficient test. Despite no statistical correlation, we observe a trend between PAI-1 concentration and LT in 15-week-old mice (Figure 16A) but not in 25-week-old mice (Figure 16B). The plaque volume also shows a trend with PAI-1 levels in both male and female 15-week-old mice (Figure 17A) and a collective trend in 25-week-old mice (Figure 17B).

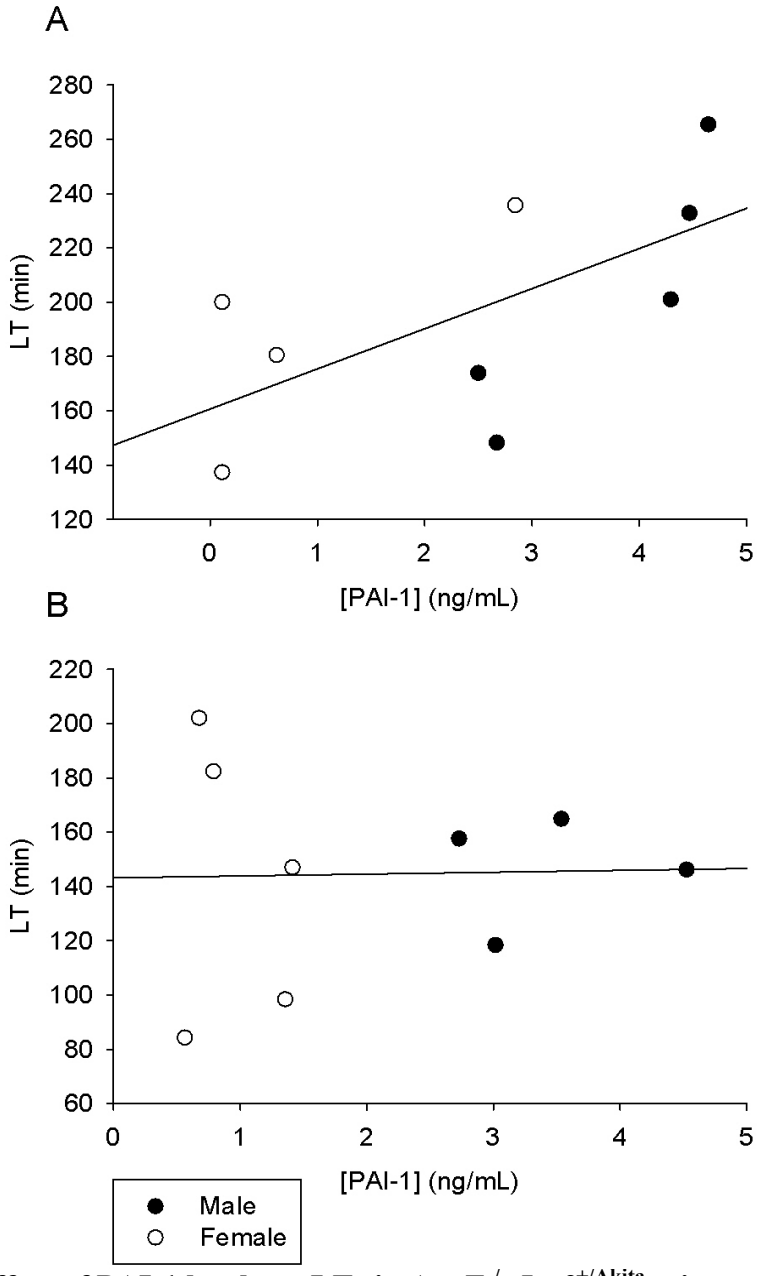

Figure 16 – Effect of PAI-1 levels on LTs in ApoE$^{-/-}$:*Ins2*$^{+/Akita}$ mice.
LTs were plotted against plasma PAI-1 levels in (A) 15-week-old and (B) 25-week-old ApoE$^{-/-}$:*Ins2*$^{+/Akita}$ mice, for both males (*closed*) and females (*open*). Using Pearson's correlation coefficient test, no correlation was observed between LTs and PAI-1 levels. The regression line represents a line of best fit. (n = at least 4).

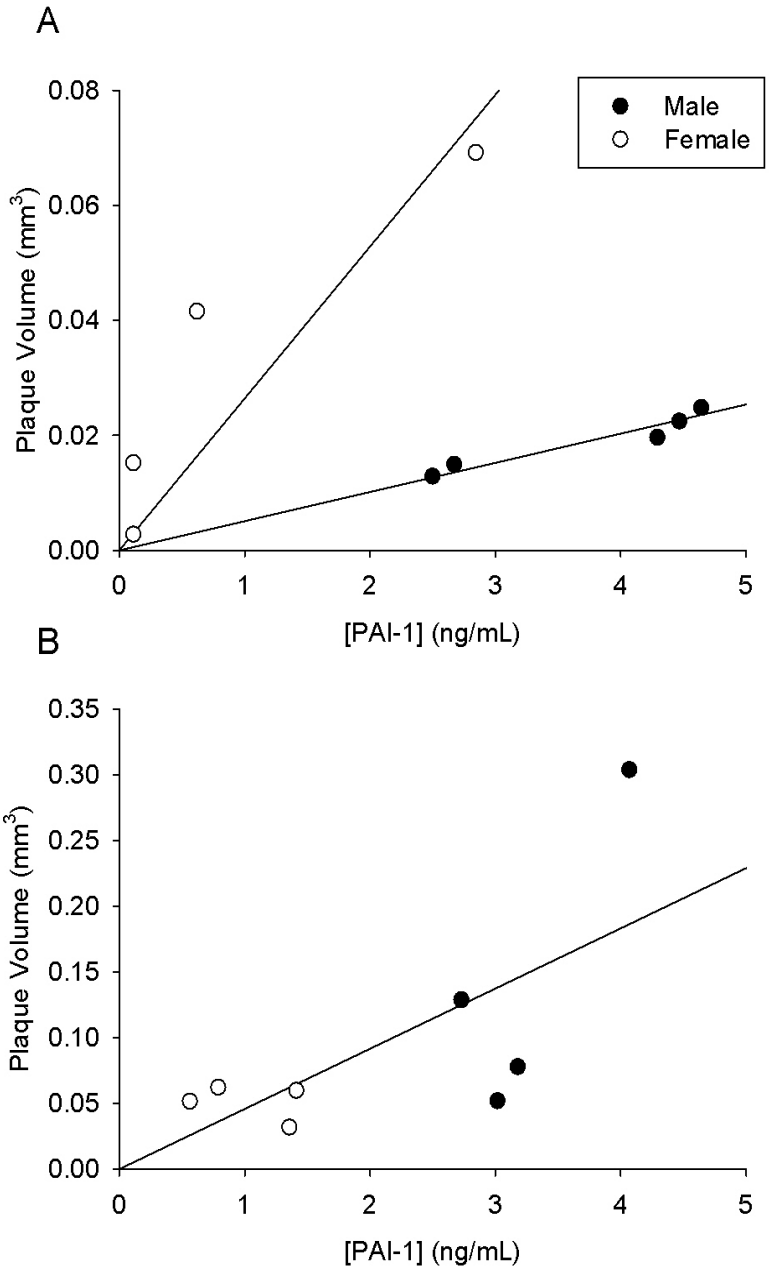

Figure 17 - Effect of PAI-1 levels on plaque volume in ApoE$^{-/-}$:*Ins2*$^{+/Akita}$ mice.
Plaque volume was plotted against plasma PAI-1 levels in (A) 15-week-old (*circle),* and (B) 25-week-old ApoE$^{-/-}$:*Ins2*$^{+/Akita}$ mice, for both males (*closed*) and females (*open*). Using Pearson's correlation coefficient test, no correlation was observed between plaque volume and PAI-1 levels. The regression line represents a line of best fit. (n = at least 4).

4 Discussion

Impaired fibrinolysis is thought to be involved in the pathogenesis of atherosclerosis and exacerbation by diabetes, but the mechanisms by which these diseases affect fibrinolysis is unclear. Our study suggest that hyperglycemia does not directly affect fibrinolysis but rather indirectly affects fibrinolysis through exacerbation of atherosclerosis. Our data also show a trend between fibrinolysis (*e.g.* LTs, TAFI and PAI-1 levels) and atherosclerosis (*e.g.* plaque volume), whereby the apparent accelerated plaque growth due to diabetes (*i.e.* hyperglycemia) results in a more pronounced effect on fibrinolysis. Therefore, our studies highlight potential novel link between fibrinolysis and atherosclerosis/diabetes.

Our preliminary findings demonstrated prolonged LTs (*i.e.* worsening fibrinolysis) in ApoE$^{-/-}$:*Ins2*$^{+/\text{Akita}}$ mice compared with both wild-type and ApoE$^{-/-}$ mice suggesting that fibrinolysis may also be impacted by both atherosclerosis and hyperglycemia in a cumulative fashion. Furthermore, preliminary data suggested that the differences were ameliorated when PTCI was included suggesting a potential role for TAFIa in the outcome. These initial findings warranted further investigation into identifying the mechanism of how atherosclerosis and hyperglycemia may affect fibrinolysis in a TAFIa-dependent manner. This potential involvement of TAFIa was not surprising given that TAFIa possesses both anti-inflammatory and antifibrinolytic properties; both properties that are the main drivers of atherosclerosis/atherothrombosis progression. Moreover, as the fibrinolytic system in both diabetes (Alzahrani & Ajjan, 2010) and atherosclerosis (Juhan-Vague & Collen, 1988) appear to be impaired, it is important to understand the mechanism

of how accelerated atherosclerosis progression due to hyperglycemia is associated with the fibrinolytic system, raising the potential of using various fibrinolytic markers as a biomarker of atherosclerosis.

When these initial findings were further investigated, using turbidity as the indicator, our data suggest that LT values are not directly correlated with the blood glucose or lipid levels. This is counter-intuitive since (a) elevated blood glucose levels are correlated with elevated fibrinogen levels (Alzahrani & Ajjan, 2010), likely as a response to a low inflammatory state, (b) clots formed from diabetic pooled fibrinogen contained a tighter fibrin network compared with controls and thus is more likely to be resistant to lysis (Alzahrani & Ajjan, 2010), and (c) PAI-1 levels are elevated, thus increased fibrinolysis impairment. In addition, elevated glucose can directly affect fibrinogen via glycation of its lysine residues, contributing to more densely packed clots that have reduced tPA and Plg binding sites (Kearney *et al*., 2017). Furthermore, glycation of plasminogen observed in diabetes directly affects fibrinolysis by decreasing plasmin generation (Ajjan *et al*., 2013). Although not statistically significant, a more in-depth analysis highlight the trend of hyperglycemia (males) resulting in higher LTs (~10-15%) compared with the age-matched normal glycemic mice (females), that is approaching significance ($p=0.083$) when assessed using a two-way ANOVA.

While there were no differences in the LTs, there was a difference observed with the inclusion of the TAFIa inhibitor, PTCI, where the 15-week-old mice had significantly longer LTs compared with 25-week-old mice in a manner that was still independent of blood glucose concentration inferred by the sex of the mice. These data suggest that (a)

fibrinolysis is more pronounced in older mice, and (b) TAFIa acts to protect these mice from age-induced hyperfibrinolytic state as evidenced by shortened LTs in the older mice with PTCI that is normalized in the absence of PTCI.

Contrary to published data indicating that elevation of lipid levels has been shown to prolong clot lysis (Edelberg & Pizzo, 1995; Anglés-Cano *et al.*, 2001), we observe that plasma cholesterol and triglyceride levels in 25-week mice may either enhance or not affect clot dissolution. It has been proposed that Lp(a) exerts a disruptive effect on fibrinolysis due to a Plg-like subunit that contains lysine binding kringle domains, which can compete with tPA and Plg binding.

Measurement of atherosclerotic plaque volume in the aortic cross sections of these mice will outline the effect diabetes has on atherosclerosis progression and any correlation with fibrinolytic parameters. We show that 25-week-old mice had significantly larger plaque volumes than 15-week-old mice independent of blood glucose concentration which is consistent with previously published data (Venegas-Pino *et al*., 2016). Although glucose has been proposed to exacerbate atherosclerosis, a two-way ANOVA indicates that the differences seen in in the plaque volume of our mice are not dependent on glucose concentration, however, this may be attributed to the small sample size (n=4-6). To investigate any trends between blood glucose concentration on individual plaque volumes, we plotted plaque volume against fasting blood glucose concentration and observed no trend at 15-weeks. At 25-weeks, however, we see a trend between blood glucose and plaque volume (Figure 16b), indicating that chronically elevated blood glucose levels may play a role in plaque volume. This is consistent with previous data, whereby, males who were

chronically hyperglycemic displayed larger plaque volumes compared to their transiently hyperglycemic female counterpart (Venegas-Pino *et al*., 2016).

TAFI zymogen levels quantified from the ELISA displayed higher concentrations to that reported by Hillmayer *et al* (Hillmayer *et al*., 2008a). Hillmayer *et al* reported average TAFI plasma concentration of 68 nM but age and sex of the mice were not described. We observe higher plasma concentration of TAFI, around 121.38 nM and 115.39 nM in 15-week-old male and female ApoE$^{-/-}$:*Ins2*$^{+/\text{Akita}}$ mice, respectively (Table 1). These higher values, however, are similar to those reported in human circulation, varying from 73 to 250 nM (Bajzar *et al*., 1995), and thus, we consider our TAFI concentration levels to be comparable to those of normal levels. TAFI concentration decreases with age, which may partly explain why older mice showed lower LTs (*i.e.* less impaired fibrinolysis) compared with the younger mice. We do not, however, observe a trend between TAFI levels and LTs for each individual mouse. Therefore, these findings are not conclusive and we would need to directly measure TAFIa levels in these mice to determine the correlation between TAFI(a) and atherosclerosis and/or diabetes.

Atherosclerosis progression is thought to start with the accumulation of lipids in the intima layer of the endothelium (Luis, 2000). Our mouse model displays a hyperlipidemia phenotype which may contribute to the severity of atherosclerosis. Therefore, we would expect the differences in lipid levels to contribute to the differences in plaque volume. At 15-weeks we observe no trend in cholesterol or triglyceride levels and plaque volume. However, at 25-weeks when mice experience chronically elevated lipid levels, there is a correlation between both cholesterol and triglyceride levels and plaque volume. This trend,

however, is more evident with 25-week males, possibly because older males displayed significantly elevated cholesterol levels compared to females. We also observe no trend between plaque volume and TAFI zymogen levels, indicating that TAFI zymogen levels may not influence atherosclerosis progression and exacerbation by diabetes, further highlighting the need for directly measuring of TAFIa levels to see its relationship with atherosclerosis and/or diabetes.

Because we show no differences in LTs based on fasting blood glucose levels and plaque volume did not correlate with blood glucose levels, we investigated if there is a trend between plaque volume and LTs. Impaired fibrinolysis seen in diabetes and atherosclerosis would suggest that longer LTs would correlate with larger plaque volumes because there is no efficient mechanism of microthrombi removal, leading to their incorporation into the plaque and increasing its overall accumulation.

Correspondingly, we show a trend between LTs and plaque volume in 15-week mice, a trend more pronounced in females. This trend, however, appeared to recede after 15-weeks for both males and females, suggesting a possible age-dependent effect of plaque volume on LT, as well as additional factors such as lipids, that may contribute to these results that are independent of fibrinolytic proteins and plaque volume. We did observe qualitative differences in these mice. Male 25-week-old ApoE$^{-/-}$:*Ins2*$^{+/\text{Akita}}$ mice are often culled due to sickness and a decline in health. Mice that survived up until the surgery presented with severe qualitative differences compared to their female counterpart, such as disorientation, hypoventilation, scruffiness, and decreased movement. Taken together, this

suggests that chronic hyperglycemia and sustained systemic inflammation may influence our results.

Diabetes represents a state of hypercoagulablity and markers of coagulation such as prothrombin F1.2 and the thrombin-antithrombin complexes are markedly elevated (Carr, 2001). Prothrombin F1.2 is cleaved from prothrombin when activated to thrombin by prothrombinase. Measurement of F1.2 provides insight into the thrombotic state of a sample, in which Ota *et al* discovered that approximately 50% of patients possess thrombosis when 300 pmol/L of F1.2 was used as a diagnostic cutoff (Ota *et al*., 2008). Furthermore, a mild correlation between F1.2, D-dimer, soluble fibrin, and thrombin-antithrombin complex was observed, indicating F1.2 as a useful variable in determining the extent of thrombosis (Ota *et al*., 2008). Therefore, we utilized this useful diagnostic tool in hopes of validating the hypercoagulable state of our diabetic and pro-atherogenic mice. Despite the varying levels of F1.2 in our mice, the differences were approaching significance ($p=0.072$) but were not statistically significant between age/sex. Moreover, two 25-week males and three 25-week female F1.2 levels were undetectable. This may indicate that these mice were either not in a prothrombotic state or F1.2 was degraded as its half-life is approximately 90 minutes (Adcock *et al*., 2006). Therefore, measurement of F1.2 in our study does not conclusively indicate a prothrombotic state in these mice, advocating the need to use another diagnostic tool such as a D-dimer test or to measure soluble fibrin.

Next, to evaluate a hypofibrinolytic state in these mice, PAI-1 levels were measured. PAI-1, a serpin released by endothelial cells, vascular smooth muscle cells, and

the liver is the main physiological regulator of fibrinolysis by forming a stable complex with tPA which then inhibits tPA-mediated Plg activation at the thrombus site (Kearney *et al*., 2017). PAI-1 levels have been shown to be an independent risk factor for cardiovascular disease and is positively correlated with HbA_{1C} levels, whereby, glucose normalization lowered PAI-1 levels (Kearney *et al*., 2017). Thus, measuring PAI-1 levels will provide us with a sense of disease severity in these mice and an elevation in PAI-1 levels could be correlated with the severity of atherosclerosis or diabetes.

The PAI-1 levels in our mice show that 15- and 25-week males had significantly elevated levels compared to their age-matched female counterpart. PAI-1 levels showed a trend with LTs in 15-week mice but subsided at 25-weeks. Similarly, we show a trend between PAI-1 levels and plaque volume in 15-week mice which subsides by 25 weeks. Taken together, these data suggest that the elevation of PAI-1 levels seen in male mice may influence or be influenced by the early onset and chronic state of diabetes and atherosclerosis. Sustained elevation in males may be attributed to the systemic effects of diabetes and atherosclerosis that exacerbate the illness of these mice and lead to a severe decline in health. It is plausible that females would not have significantly elevated PAI-1 levels, as both diabetes and atherosclerosis in these mice are not as severe as the males. Eitsman *et al* outline that their PAI-$1^{-/-}$:$ApoE^{-/-}$ mice develop similar atherosclerotic lesions in the aortic arch when compared to $ApoE^{-/-}$ and that PAI-$1^{-/-}$:$ApoE^{-/-}$ display protection from atherosclerosis advancement at the site of the carotid bifurcation (Eitzman *et al.*, 2000). This suggests that there is an important role for PAI-1 at locations where blood flow is more turbulent, which may be the inhibition of clot dissolution. They then stained for

fibrinogen/fibrin and noticed that there was a marked increase in fibrinogen/fibrin staining in atherosclerotic lesions at the carotid bifurcation compared to the aortic arch (Eitzman *et al.*, 2000). Therefore, there may be critical differences in the pathogenesis of atherosclerosis at different locations of the vasculature, and that PAI-1 may be exacerbating this disease at different areas. Confining our study to the aortic arch may be limiting our investigation of the correlation between atherosclerosis, diabetes, and fibrinolysis considering there are differences in atherosclerosis progression at varying sites of the vascular tree and that parameters we measured may be affecting disease progression at different sites in the vasculature.

Our ApoE$^{-/-}$:*Ins2*$^{+/\text{Akita}}$ model and methods of investigating fibrinolysis may be unsuitable to study the effects of atherosclerosis and diabetes on fibrinolysis, and whether there is a role for TAFIa. Because the primary role of TAFIa is thought to be involved in fibrinolysis and its secondary role in inflammation, it is plausible to investigate whether it is involved in the removal of microthrombi/thrombi that form within or on ruptured plaques. This is quite difficult, despite our use of the ApoE$^{-/-}$ mouse model, as there are no readily available atherothrombosis mouse models. To fully investigate the role of TAFI(a) in atherosclerosis and exacerbation by diabetes, a mouse dedicient in both TAFI and ApoE that develops diabetes is necessary. Beppu *et al.* describe a TAFI$^{-/-}$:ApoE$^{-/-}$ mouse that develops diabetes via the administration of streptozotocin (Stz) (Beppu *et al*., 2010). They show that these mice readily develop hepatic tumors and have no difference in the activation of their coagulation system. Stz is a compound used as a chemotherapy agent to treat β-cell carcinoma (Graham *et al*., 2011). Stz can be administrated in low or high dose

and as a result, damages pancreatic β cells leading to hyperglycemia. Stz, however, has well-known side effects that include liver and kidney toxicity. Therefore, using this diabetic model may not be ideal, considering the use of Stz with the TAFI$^{-/-}$:ApoE$^{-/-}$ mouse model would result in hepatic tumors. For that reason, to accurately assess the contribution of TAFI(a) in atherosclerosis progression and exacerbation by diabetes, we will need to develop a TAFI$^{-/-}$:ApoE$^{-/-}$:*Ins2*$^{+/Akita}$ triple mutant mouse.

Focusing our studies on the aortic arch and carotid artery may also be limiting the overall effects of this systemic inflammation and chronic hyperglycemia. At 25-weeks of age, male ApoE$^{-/-}$:*Ins2*$^{+/Akita}$ exhibit a severe decline in health. The decline in health may be attributed to chronic hyperglycemia and systemic inflammation, resulting in severe atherosclerosis that is not solely localized to the carotid artery. The variable LTs combined with plaque volumes in the 25-week-old males may suggest that the effects of hyperglycemia and systemic inflammation are occurring elsewhere in the system, meanwhile we are limited to the aortic arch. Our observation of elevated PAI-1 levels in male mice may also suggest severe progression of atherosclerosis that is not localized to the aortic arch but at the carotid bifurcation (Eitzman, 2000). Lesion progression has been shown to occur in both renal arteries as well as the pulmonary artery, and in older mice the lesions were observed in femoral, iliac, abdominal, and proximal coronary arteries (Nakashima *et al*., 1994). Therefore, simply investigating the carotid artery and aortic arch may be limiting the effects of hyperglycemia and atherosclerosis to one area, when in fact the effects are systemic and non-localized. It is uncertain whether fibrinolysis is only affected in the aortic arch and carotid artery, so opening this study to investigating other

areas that are prone to lesions may be beneficial in determining any correlation atherosclerosis and exacerbation by diabetes have on fibrinolysis and the role of TAFIa in these disease states.

Currently, there are no studies investigating the relationship between atherosclerosis, diabetes and fibrinolysis in ApoE$^{-/-}$:*Ins2*$^{+/Akita}$. Our study shows that diabetes may accelerate atherosclerosis as observed with higher PVs in males (hyperglycemia) compared to females (normal glycaemia), especially at 25-weeks. We also show that when analyzed more closely, LTs show a trend with PVs, outlining a correspondence between diabetes and atherosclerosis in in ApoE$^{-/-}$:*Ins2*$^{+/Akita}$ mice. Plasma lipid levels show a trend with plaque volume, suggesting a possible diagnostic marker for determining the severity of atherosclerosis. Concurrently, we show a trend between PAI-1 levels and plaque volume. This indicates an indirect relationship between plasma lipid levels, PAI-1 levels, and plaque volume with clot lysis. Because there is a trend with lipid and PAI-1 levels with plaque volume, and there is a trend between plaque volume and LTs (*i.e.* fibrinolysis), we can infer that PAI-1 and lipid levels play a role in the fibrinolytic system in the ApoE$^{-/-}$:*Ins2*$^{+/Akita}$ mouse model. A chronic inflammatory disease like atherosclerosis may support an environment for sustained elevation of TAFIa as well as other coagulation and fibrinolytic proteins. Further investigation into coagulation and fibrinolytic proteins may also provide us with a better understanding of the mechanism of impaired fibrinolysis in atherosclerosis and diabetes, as well as potential biomarkers for disease severity. Confirmation will aid in early disease detection, identifying the severity of the disease, and possible treatment.

5 Future directions

To investigate the correlation of atherosclerosis and exacerbation by diabetes have on fibrinolysis and if this is TAFI(a)-dependent, we will use our in-house assay to quantify TAFIa levels in the plasma samples of these mice. Furthermore, we will characterize time-course activation of TAFI and plasminogen in ApoE$^{-/-}$:*Ins2*$^{+/Akita}$ and WT plasma to assess if atherosclerosis and diabetes affect TAFI and plasminogen activation. Furthermore, we will characterize additional fibrinolytic markers such as fibrinogen levels, soluble fibrin, D-dimer, thrombin-antithrombin and plasmin-antiplasmin complexes. We will also conduct further histological analyses to determine endothelium activation and macrophage recruitment to see if there is a relationship with fibrinolytic markers and atherosclerosis progression.

To elucidate the role of TAFIa in atherosclerosis progression and exacerbation in diabetes, we will generate TAFI/ApoE double knockout and TAFI$^{-/-}$:ApoE$^{-/-}$:*Ins2*$^{+/Akita}$ triple mutant mice. We will compare the atherosclerotic plaques in these mice to identify if TAFIa plays a role in plaque development with and without diabetes and assess the fibrinolytic and atherosclerotic parameters in the absence of TAFIa in atherosclerosis and diabetes.

6 References

Adcock DM, Bethel MA, Macy PA, *et al*. *Coagulation Handbook.* Esoterix Coagulation; 2006.

Alessi, M. C., & Juhan-Vague, I. (2006, October). PAI-1 and the metabolic syndrome: Links, causes, and consequences. *Arteriosclerosis, Thrombosis, and Vascular Biology*.

Alzahrani, S. H., & Ajjan, R. a. (2010). Coagulation and fibrinolysis in diabetes. *Diabetes & Vascular Disease Research: Official Journal of the International Society of Diabetes and Vascular Disease*, *7*(4), 260–273.

Anglés-Cano, E., Díaz, A. D. L. P., & Loyau, S. (2010). Inhibition of Fibrinolysis by Lipoprotein(a). *Annals of the New York Academy of Sciences*, *936*(1), 261–275.

Aronson, D., & Rayfield, E. J. (2002, April 8). How hyperglycemia promotes atherosclerosis: Molecular mechanisms. *Cardiovascular Diabetology*.

Bajzar, L., Manuel, R., & Nesheim, M. E. (1995). Purification and characterization of TAFI, a thrombin-activable fibrinolysis inhibitor. *Journal of Biological Chemistry*, *270*(24), 14477–14484.

Bajzar, L., Nesheim, M. E., & Tracy, P. B. (1996). The profibrinolytic effect of activated protein C in clots formed from plasma is TAFI-dependent. *Blood*, *88*(6), 2093–2100

Barlovic, D. P., Soro-Paavonen, A., & Jandeleit-Dahm, K. A. M. (2011). RAGE biology, atherosclerosis and diabetes. *Clinical Science*, *121*(2), 43–55.

Barthel, D., Schindler, S., & Zipfel, P. F. (2012). Plasminogen is a complement inhibitor. *Journal of Biological Chemistry*, *287*(22), 18831–18842.

Beppu, T., Gil-Bernabe, P., Boveda-Ruiz, D., D'alessandro-Gabazza, C., Matsuda, Y., Toda, M., … Takei, Y. (2010). High incidence of tumors in diabetic thrombin activatable fibrinolysis inhibitor and apolipoprotein E double-deficient mice. *Journal of Thrombosis and Haemostasis*, *8*(11), 2514–2522.

Bowes, A. J., Pichna, B. A., Shi, Y., Khan, M. I., & Werstuck, G. H. (2009). Evidence Supporting a Role for Endoplasmic Reticulum Stress in the Development of Atherosclerosis in a Hyperglycaemic Mouse Model. *Antioxidants & Redox Signaling*, *11*(9), 2289–2298.

Brett, J., Schmidt, A. M., Yan, S. D., Zou, Y. S., Weidman, E., Pinsky, D., … Shaw, A. (1993). Survey of the distribution of a newly characterized receptor for advanced

glycation end products in tissues. *The American Journal of Pathology*, *143*(6), 1699–712.

Broze, G. J., & Higuchi, D. a. (1996). Coagulation-dependent inhibition of fibrinolysis: role of carboxypeptidase-U and the premature lysis of clots from hemophilic plasma. *Blood*, *88*(10), 3815–23.

Bucala, R., Makita, Z., Vega, G., Grundy, S., Koschinsky, T., Cerami, A., & Vlassara, H. (1994). Modification of low density lipoprotein by advanced glycation end products contributes to the dyslipidemia of diabetes and renal insufficiency. *Proc Natl Acad Sci U S A*, *91*(20), 9441–9445.

Campbell, W., & Okada, H. (1989). An arginine specific carboxypeptidase generated in blood during coagulation or inflammation which is unrelated to carboxypeptidase N or its subunits. *Biochemical and Biophysical Research Communications*, *162*(3), 933–939.

Canadian Diabetes Association. Types of Diabetes. 2017, from http://diabetes.ca/about-diabetes/types-of-diabetes

Cale, J., & Lawrence, D. (2007). Structure-Function Relationships of Plasminogen Activator Inhibitor-1 and Its Potential as a Therapeutic Agent. *Current Drug Targets*, *8*(9), 971–981.

Carpenter SL, Mathew P. Alpha2-antiplasmin and its deficiency: fibrinolysis out of balance. Haemophilia 2008;14:1250-4.

Carr, M. E. (2001). Diabetes mellitus: A hypercoagulable state. *Journal of Diabetes and Its Complications*, *15*(1), 44–54.

Centers for Disease Control and Prevention. Diabetes at Work. 2016, from https://www.cdc.gov/diabetes/diabetesatwork/diabetes-basics/what.html

Cesari, M., Pahor, M., & Incalzi, R. A. (2010). Plasminogen activator inhibitor-1 (PAI-1): A key factor linking fibrinolysis and age-related subclinical and clinical conditions. *Cardiovascular Therapeutics*.

Chait, A., & Bornfeldt, K. E. (2009). Diabetes and atherosclerosis: is there a role for hyperglycemia? *Journal of Lipid Research*, *50*(Supplement), S335–S339.

Chapin, J. C., & Hajjar, K. A. (2015). Fibrinolysis and the control of blood coagulation. *Blood Reviews*. Churchill Livingstone.

Collen, D., & Juhan-Vague, I. (1988). Fibrinolysis and atherosclerosis. *Seminars in Thrombosis and Hemostasis*.

Collet, J. P., Allali, Y., Lesty, C., Tanguy, M. L., Silvain, J., Ankri, A., … Montalescot, G. (2006). Altered fibrin architecture is associated with hypofibrinolysis and premature coronary atherothrombosis. *Arteriosclerosis, Thrombosis, and Vascular Biology*, *26*(11), 2567–2573.

Comai, K., Feldman, D. L., Goldstein, A. L., & Hamilton, J. G. (1985). Atherosclerosis: An overview. *Drug Development Research*, *6*(2), 113–125.

Cybulsky, M. I., Iiyama, K., Li, H., Zhu, S., Chen, M., Iiyama, M., … Milstone, D. S. (2001). A major role for VCAM-1, but not ICAM-1, in early atherosclerosis. *Journal of Clinical Investigation*, *107*(10), 1255–1262.

Declerck, P. J. (2011). Thrombin activatable fibrinolysis inhibitor. *Hamostaseologie*.

Diabetes.co.uk. (2014). Blood Sugar Level Ranges. *Diabetes.Co.Uk*, 9–12. Retrieved from http://www.diabetes.co.uk/diabetes_care/blood-sugar-level-ranges.html

Duguid, J. B. (1946). Thrombosis as a factor in the pathogenesis of coronary atherosclerosis. *J.Pathol.Bacteriol., 58,* 207-212.

Eaton, D. L., Malloy, B. E., Tsai, S. P., Henzel, W., & Drayna, D. (1991). Isolation, molecular cloning, and partial characterization of a novel carboxypeptidase B from human plasma. *The Journal of Biological Chemistry*, *266*, 21833–21838.

Edelberg, J. M., Pizzo, S. V. (1995). Lipoprotein (a) in the regulation of fibrinolysis. *Journal of Atherosclerosis and Thrombosis,* 2 Suppl 1:S5-7

Edelberg, J. M., Reilly, C. F., & Pizzo, S. V. (1991). The inhibition of tissue type plasminogen activator by plasminogen activator inhibitor-1: The effects of fibrinogen, heparin, vitronectin, and lipoprotein(a). *Journal of Biological Chemistry*, *266*(12), 7488–7493.

Eitzman, D. T., Westrick, R. J., Xu, Z., Tyson, J., & Ginsburg, D. (2000). Plasminogen activator inhibitor-1 deficiency protects against atherosclerosis progression in the mouse carotid artery. *Blood*, *96*(13), 4212–5.

Fiorentino, T. V., Prioletta, A., Zuo, P., & Folli, F. (2013). Hyperglycemia-induced oxidative stress and its role in diabetes mellitus related cardiovascular diseases. *Current Pharmaceutical Design*, *19*(32), 5695–703.

Flier, J. S., Underhill, L. H., Brownlee, M., Cerami, A., & Vlassara, H. (1988). Advanced Glycosylation End Products in Tissue and the Biochemical Basis of Diabetic Complications. *New England Journal of Medicine*, *318*(20), 1315–1321.

Foley, J. H., Kim, P. Y., Mutch, N. J., & Gils, A. (2013). Insights into thrombin activatable fibrinolysis inhibitor function and regulation. *Journal of Thrombosis & Haemostasis, 11 Suppl 1,* 306-315.

Fredenburgh, J. C., & Nesheim, M. E. (1992). Lys-plasminogen is a significant intermediate in the activation of Glu- plasminogen during fibrinolysis in vitro. *Journal of Biological Chemistry*, *267*(36), 26150–26156.

Graham, M. L., Janecek, J. L., Kittredge, J. A., Hering, B. J., & Schuurman, H. J. (2011). The streptozotocin-induced diabetic nude mouse model: differences between animals from different sources. *Comparative medicine*, *61*(4), 356-360.

Hillmayer, K., Brouwers, E., Leon-Tamariz, F., Meijers, J. C., Marx, P. F., Declerck, P. J. *et al*. (2008a). Development of sandwich-type ELISAs for the quantification of rat and murine thrombin activatable fibrinolysis inhibitor in plasma. *Journal of Thrombosis & Haemostasis, 6,* 132-138.

Hillmayer, K., Ceresa, E., Vancraenenbroeck, R., Declerck, P. J., & Gils, A. (2008b). Conformational (in)stability of rat vs. human activated thrombin activatable fibrinolysis inhibitor. *Journal of Thrombosis & Haemostasis, 6,* 1426-1428.

Horrevoets, A. J. G., Pannekoek, H., & Nesheim, M. E. (1997). A steady-state template model that describes the kinetics of fibrin- stimulated [Glu1]- and [Lys78] plasminogen activation by native tissue- type plasminogen activator and variants that lack either the finger or kringle-2 domain. *Journal of Biological Chemistry*, *272*(4), 2183–2191.

Hoylaerts, M., Rijken, D. C., Lijnen, H. R., & Collen, D. (1982). Kinetics of the activation of plasminogen by human tissue plasminogen activator. Role of fibrin. *Journal of Biological Chemistry*, *257*(6), 2912–2919.

Jawień, J., Nastałek, P., & Korbut, R. (2004, September). Mouse models of experimental atherosclerosis. *Journal of Physiology and Pharmacology*.

Jörneskog G, Egberg N, Fagrell B, Fatah K, Hessel B, Johnsson H, *et al*. Altered properties of the fibrin gel structure in patients with IDDM. *Diabetologia* 1996; 39: 1519–1523

Kanter, J. E., & Bornfeldt, K. E. (2013, March). Inflammation and diabetes-accelerated atherosclerosis: Myeloid cell mediators. *Trends in Endocrinology and Metabolism*.

Katsuda, Y., Ohta, T., Shinohara, M., Bin, T., & Yamada, T. (2013). Diabetic mouse models. *Open Journal of Animal Sciences*, *03*(04), 334–342.

Kearney, K., Tomlinson, D., Smith, K., & Ajjan, R. (2017). Hypofibrinolysis in diabetes: A therapeutic target for the reduction of cardiovascular risk. *Cardiovascular Diabetology*. BioMed Central Ltd.

Khan, M. I., Pichna, B. A., Shi, Y., Bowes, A. J., & Werstuck, G. H. (2009). Evidence supporting a role for endoplasmic reticulum stress in the development of atherosclerosis in a hyperglycaemic mouse model. *Antioxid Redox Signal*, *11*(9), 2289–2298.

Kim, P. Y. G., Foley, J., Hsu, G., Kim, P. Y., & Nesheim, M. E. (2008). An assay for measuring functional activated thrombin-activatable fibrinolysis inhibitor in plasma. *Analytical Biochemistry*, *372*(1), 32–40.

Kim, P. Y., Stewart, R. J., Lipson, S. M., & Nesheim, M. E. (2007). The relative kinetics of clotting and lysis provide a biochemical rationale for the correlation between elevated fibrinogen and cardiovascular disease. *Journal of Thrombosis and Haemostasis*, *5*(6), 1250–1256.

King, G. L., & Loeken, M. R. (2004). Hyperglycemia-induced oxidative stress in diabetic complications. *Histochemistry and Cell Biology*.

Lee, T. S., Saltsman, K. A., Ohashi, H., & King, G. L. (1989). Activation of protein kinase C by elevation of glucose concentration: proposal for a mechanism in the development of diabetic vascular complications. *Proc Natl Acad Sci U S A*, *86*(13), 5141–5145.

Lusis, A. J. (2000). Atherosclerosis. *Nature, 407,* 233-241.

Marx, P. F., Brondijk, T. H. C., Plug, T., Romijn, R. A., Hemrika, W., Meijers, J. C. M., & Huizinga, E. G. (2008). Crystal structures of TAFI elucidate the inactivation mechanism of activated TAFI: A novel mechanism for enzyme autoregulation. *Blood*, *112*(7), 2803–2809.

Ma, Y., Wang, W., Zhang, J., Lu, Y., Wu, W., Yan, H., & Wang, Y. (2012). Hyperlipidemia and atherosclerotic lesion development in Ldlr-deficient mice on a long-term high-fat diet. *PloS One*, *7*(4). https://doi.org/10.1371/journal.pone.0035835

Matsuo, O., Lijnen, H. R., Ueshima, S., Kojima, S., & Smyth, S. S. (2007). A guide to murine fibrinolytic factor structure, function, assays, and genetic alterations. *Journal of Thrombosis & Haemostasis, 5,* 680-689.

Mosnier, L. O. (2003). Identification of thrombin activatable fibrinolysis inhibitor (TAFI) in human platelets. *Blood*, *101*(>12), 4844–4846.

Mosesson, M. W. (2005). Fibrinogen and fibrin structure and functions. In *Journal of Thrombosis and Haemostasis* (Vol. 3, pp. 1894–1904). https://doi.org/10.1111/j.1538-7836.2005.01365.x

Ni, R., Peleg, T., & Gross, P. L. (2012). Atorvastatin delays murine platelet activation in vivo even in the absence of endothelial NO synthase. *Arterioscler.Thromb.Vasc.Biol., 32,* 2609-2615.

Nakashima, Y., Plump, A. S., Raines, E. W., Breslow, J. L., & Ross, R. (1994). ApoE-deficient mice develop lesions of all phases of atherosclerosis throughout the arterial tree. *Arteriosclerosis and Thrombosis, 14,* 133-140.

Norrman, B., Wallén, P., & Rånby, M. (1985). Fibrinolysis mediated by tissue plasminogen activator: Disclosure of a kinetic transition. *European Journal of Biochemistry*, *149*(1), 193–200.

Ota, S., Wada, H., Abe, Y., Yamada, E., Sakaguchi, A., Nishioka, J., … Nobori, T. (2008). Elevated levels of prothrombin fragment 1 + 2 indicate high risk of thrombosis. *Clinical and Applied Thrombosis/Hemostasis*, *14*(3), 279–285.

Otsuka, F., Yasuda, S., Noguchi, T., & Ishibashi-Ueda, H. (2016). Pathology of coronary atherosclerosis and thrombosis. *Cardiovascular Diagnosis and Therapy*, *6*(4), 396–408.

Pandolfi, A., Giaccari, A., Cilli, C., Alberta, M. M., Morviducci, L., De Filippis, E. A., Consoli, A. (2001). Acute hyperglycemia and acute hyperinsulinemia decrease plasma fibrinolytic activity and increase plasminogen activator inhibitor type 1 in the rat. *Acta Diabetologica*, *38*(2), 71–76.

Pendse, A. A., Arbones-mainar, J. M., Johnson, L. A., Altenburg, M., & Maeda, N. (2011). ApoE Knock-out and Knock-in Mice: Atherosclerosis, Metabolic Syndrome, and Beyond. *Journal of Lipid Research*, 1–18.

Rezzani, R., Bonomini, F., Tengattini, S., Fabiano, A., & Bianchi, R. (2008). Atherosclerosis and oxidative stress. *Histology and Histopathology*, *23*(3), 381–390.

Rijken, D. C., & Lijnen, H. R. (2009). New insights into the molecular mechanisms of the fibrinolytic system. *Journal of Thrombosis and Haemostasis : JTH*, *7*(1), 4–13.

Rosenfeld, M. A., Bychkova, A. V., Shchegolikhin, A. N., Leonova, V. B., Kostanova, E. A., Biryukova, M. I., … Konstantinova, M. L. (2016). Fibrin self-assembly is adapted to oxidation. *Free Radical Biology and Medicine*, *95*, 55–64.

Ruggeri, Z. M., & Jackson, S. P. (2013). Platelet Thrombus Formation in Flowing Blood. In *Platelets* (pp. 399–423). Elsevier Inc.

Sadler, J. E. (1997). Thrombomodulin structure and function. In *Thrombosis and Haemostasis*(Vol. 78, pp. 392–395).

Schmidt, A. M., Hori, O., Brett, J., Yan, S. D., Wautier, J. L., & Stern, D. (1994). Cellular receptors for advanced glycation end products. Implications for induction of oxidant stress and cellular dysfunction in the pathogenesis of vascular lesions. Arteriosclerosis, Thrombosis, and Vascular Biology, 14(10), 1521–1528.

Schneider, M., Brufatto, N., Neill, E., & Nesheim, M. (2004). Activated Thrombin-activatable Fibrinolysis Inhibitor Reduces the Ability of High Molecular Weight Fibrin Degradation Products to Protect Plasmin from Antiplasmin. *Journal of Biological Chemistry*, *279*(14), 13340–13345.

Singh, V. P., Bali, A., Singh, N., & Jaggi, A. S. (2014). Advanced glycation end products and diabetic complications. *Korean Journal of Physiology and Pharmacology*. Korean Physiological Soc. and Korean Soc. of Pharmacology.

Sobel, B. E. (2003). Fibrinolysis and diabetes. *Frontiers in Bioscience: A Journal and Virtual Library*, *8*, d1085-92.

Soro-Paavonen, A., Watson, A. M. D., Li, J., Paavonen, K., Koitka, A., Calkin, A. C., … Jandeleit-Dahm, K. A. (2008). Receptor for advanced glycation end products (RAGE) deficiency attenuates the development of atherosclerosis in diabetes. *Diabetes*, *57*(9), 2461–2469.

Spronk, H. M. H., van der Voort, D., & ten Cate, H. (2004). Blood coagulation and the risk of atherothrombosis: A complex relationship. *Thrombosis Journal*.

Steinbrecher, U. P., & Witztum, J. L. (1984). Glucosylation of low-density lipoproteins to an extent comparable to that seen in diabetes slows their catabolism. *Diabetes*, *33*(2), 130–134.

Tegos, T. J., Kalodiki, E., Sabetai, M. M., & Nicolaides, A. N. (2001). The genesis of atherosclerosis and risk factors: a review. *Angiology, 52,* 89-98.

The Jackson Laboratory Mouse Strain Datasheet. (2018). *C57BL/6-Ins2Akita/J Mouse Datasheet*. [online] Available at: https://www.jax.org/strain/003548 [Accessed January, 2019].

Undas, A., Wiek, I., Stêpień, E., Zmudka, K., & Tracz, W. (2008). Hyperglycemia is associated with enhanced thrombin formation, platelet activation, and fibrin clot resistance to lysis in patients with acute coronary syndrome. *Diabetes Care*, *31*(8), 1590–1595.

Venegas-Pino, D. E., Shi, Y., Khan, M. I., Banko, N., & Werstuck, G. H. (2013). Quantitative Analysis and Characterization of Atherosclerotic Lesions in the Murine Aortic Sinus. *Journal of Visualized Experiments*, (82).

Venegas-Pino, Daniel E., *et al*. (2016). Sex-Specific Differences in an ApoE−/−: Ins2+/Akita Mouse Model of Accelerated Atherosclerosis. *The American journal of pathology,* 186:1 67-77.

Vlassara, H., & Palace, M. R. (2002). Diabetes and advanced glycation endproducts. *J Intern Med*, *251*(2), 87–101.

Wang, W., Hendriks, D. F., & Scharp??, S. S. (1994). Carboxypeptidase U, a plasma carboxypeptidase with high affinity for plasminogen. *Journal of Biological Chemistry*, *269*(22), 15937–15944.

Wautier, J. L., Zoukourian, C., Chappey, O., Wautier, M. P., Guillausseau, P. J., Cao, R., … Schmidt, A. M. (1996). Receptor-mediated endothelial cell dysfunction in diabetic vasculopathy. Soluble receptor for advanced glycation end products blocks hyperpermeability in diabetic rats. *J Clin Invest*, *97*(1), 238–243.

Werstuck, G. H., Khan, M. I., Femia, G., Kim, A. J., Tedesco, V., Trigatti, B., & Shi, Y. (2006). Glucosamine-induced endoplasmic reticulum dysfunction is associated with accelerated atherosclerosis in a hyperglycemic mouse model. *Diabetes*, *55*(1), 93–101.

World Health Organization. Diabetes. 2013, from https://web.archive.org/web/20140414092858/http://www.who.int/mediacentre/factsheets/fs312/en/

Yasar Yildiz, S., Kuru, P., Toksoy Oner, E., & Agirbasli, M. (2014). Functional stability of plasminogen activator inhibitor-1. *Scientific World Journal*. Hindawi Publishing Corporation.

Zadelaar, Susanne, *et al*. (2007). Mouse models for atherosclerosis and pharmaceutical modifiers. *Arteriosclerosis, thrombosis, and vascular biology,* 27:8 1706- 1721.

Zhang, S. H., Reddick, R. L., Piedrahita, J. A., & Maeda, N. (1992). Spontaneous hypercholesterolemia and arterial lesions in mice lacking apolipoprotein E. *Science*, *258*(5081), 468–471.

7 Appendix

Includes:

Kim, P. Y., Di Giuseppantonio, L. R., Wu, C., Douketis, J. D., Gross, P. L. (2019). An assay to measure levels of factor Xa inhibitors in blood and plasma. *J Thromb Haemost* 17(7), 1153-1159.

My role included measuring the anti-factor Xa direct oral anticoagulant levels in plasma samples from patients enrolled in the PAUSE study, as well as preparing and editing the manuscript. For this work, I was funded by the Canadian Venous Thromboembolism Clinical Trials and Outcomes Research (CanVECTOR) Network Studentship Award.

An assay to measure levels of factor Xa inhibitors in blood and plasma

Paul Y. Kim[1,2,3], Luca R. Di Giuseppantonio[1,2], Chengliang Wu[1,3], James D. Douketis[1,3], Peter L. Gross[1,2,3]

[1]Thrombosis and Atherosclerosis Research Institute, Hamilton, Ontario, Canada; Departments of [2]Medical Sciences and [3]Medicine, McMaster University, Hamilton, Ontario, Canada.

Running Title: *Quantifying DOACs in plasma and blood*

Correspondence to:
Paul Y. Kim, Ph.D.
Thrombosis and Atherosclerosis Research Institute
237 Barton Street East, Hamilton, Ontario, L8L 2X2
Tel: 905-521-2100 x40781
Fax: 905-575-2646
E-mail: paul.kim@taari.ca

Keywords: DOACs, quantification, inhibition, plasma, blood

Essentials:

- Direct oral anticoagulants (DOAC) are used for stroke and venous thromboembolism prevention.
- We report a new assay that measures anti-factor Xa DOACs levels in plasma and whole blood.
- Rivaroxaban and apixaban can be accurately quantified below trough levels.
- The ease and accuracy of the assay demonstrates its potential for point-of-care applications.

Summary

Background: Rivaroxaban and apixaban are the most commonly used anti-factor (F) Xa direct oral anticoagulants (DOAC), with indications for prevention of stroke in non-valvular atrial fibrillation as well as treatment and prevention of venous thromboembolism. However, lacking is accessibility to a detection method that is able to quantify low levels of anti-FXa DOACs. Objective: We report a new assay that measures anti-FXa DOACs levels in plasma and whole blood. Methods: This is achieved by the use of a prothrombin derivative that is labeled with a fluorescent probe (Flu-II), which then acts as the macromolecular substrate to measure residual FXa activity. Flu-II cleavage is then initiated by the addition of a solution containing FXa, FVa, and PCPS vesicles with calcium, in the presence of hirudin to prevent feedback activity by the native thrombin generated. Flu-II cleavage is monitored by fluorescence in real-time where the initial rate of fluorescence change is inversely proportional to DOAC levels. Results: In plasma systems, the assay demonstrates dose-response between 0 and 5 nM rivaroxaban and between 0 and 10 nM apixaban. Corn trypsin inhibitor did not affect this assay. With individual plasma samples, the assay showed excellent consistency and reproducibility. From 2 µL of whole blood, the assay showed dose-response between 0 and 2 nM of DOACs in the final mixture of 100 µL, thus representing up to 100 nM in circulating blood. Conclusion: The assay is ideal for rapidly and accurately measuring DOAC levels in plasma and blood, demonstrating its potential for point-of-care applications.

Introduction

A new class of anticoagulant drugs often referred to as direct oral anticoagulants (DOAC) are being used more frequently in the prevention and treatment of arterial and venous thrombosis [1]. DOACs are classified as targeting either thrombin or factor (F) Xa. As such, with the increased use of anti-FXa DOACs, it is becoming more important to be able, at certain times, to efficiently and accurately measure the levels of these agents in the blood of patients [1-3]. Rivaroxaban and apixaban are two of the more commonly used anti-FXa DOACs.

A distinct advantage of DOACs is that, unlike warfarin, on-going monitoring of anticoagulation is not as necessary due to their predictable pharmacokinetics and bioavailability; thus they have been adopted despite limited ability to measure their levels. However, in some situations accurate quantitation of anti-FXa DOACs is needed, for instance, when a patient stops anticoagulation in preparation for surgery or when a patient is experiencing a bleeding or thrombotic event [1,4]. Current guidelines by different organizations offer conflicting recommendations of when patients should stop their anti-FXa DOAC which results in miscommunication that often leads to delayed patient care that wastes time, money, and healthcare resources [5-8].

The inability to correlate the levels of anti-FXa DOACs with bleeding risk remains the largest reason for disparate recommendations of fixed time post-cessation of anticoagulation prior to high-bleed risks procedures, including epidural anaesthesia [4,6,7]. The inability to accurately measure very low levels of these anti-FXa DOACs [9-11] contributes to this problem. Situations where DOACs may not have predictable

pharmacokinetics such as extremes in body weight, liver or renal impairment, and drug interactions further complicate the problem [1,5,6]. Currently there are two major methods used to accurately quantify levels of anti-FXa DOAC levels in the blood of patients: a chromogenic substrate enzyme assay [12], and a method that utilizes high-performance liquid chromatography (HPLC) to isolate and quantify DOACs [13]. There are two major drawbacks on these methods. The HPLC assay is only done in research facilities, thus not practical for use as a diagnostic tool in a clinical setting; however, it is accurate to very low levels. The chromogenic assay needs a skilled technician in a specialty laboratory to perform, and lacks sensitivity, as the assay cannot accurately detect DOACs less than 20 ng/mL (~45 nM) [2,9,10,14].

Here, we describe a simple assay that is sensitive to levels of anti-FXa DOACs below the current limit of detection of the chromogenic assays. It demonstrates dose-response between 0 and 5 nM for rivaroxaban and between 0 and 10 nM for apixaban when measured in plasma. In addition, levels of DOACs can be measured in whole blood, suggesting its potential for use as a point-of-care assay.

Experimental Procedures

Materials – Human FXa and FVa were purchased from Haematologic Technologies Inc. (Essex Junction, VT, USA). QuikChange Lightening Site-Directed Mutagenesis Kit was purchased from Agilent Technologies (Santa Clara, CA, USA). QIAprep® Spin Miniprep Kit and Plasmid Maxi Kit were purchased from Qiagen (Hilden, Germany). Lipofectamine® 3000 Transfection Kit was purchased from Life Technologies-Invitrogen

(Carlsbad, CA, USA). Baby hamster kidney cells and the pNUT vector, used for mammalian expression, were kindly provided by Dr. Ross MacGillivray (University of British Columbia). Methotrexate (Mayne Pharma Inc., Montreal, Quebec Canada) and Vitamin K_1 were purchased from Hamilton General Hospital. Q-Sepharose Fast Flow anion-exchange resin and Mono-Q HR 5/5 column were obtained from GE Healthcare (Burlington, Ontario Canada). Gibco® D-MEM/F-12 media, newborn calf serum and Opti-MEM I media, 0.5% Trypsin-EDTA and Antibiotic-Antimycotic solution were purchased from Thermo Fisher Scientific (Carlsbad, CA, USA). Phosphatidyl-L-serine, phosphatidyl-L-choline, and XAD-2 resin were obtained from Sigma. Matched-Pair Antibody Set for ELISA of Human Prothrombin Antigen, was purchased from Affinity Biologicals Inc. (Ancaster, ON, Canada). 5-iodoacetamidofluorescein (5-IAF) was purchased from Marker Gene Technologies Inc. (Eugene, OR, USA). The recombinant prothrombin with a single mutation of the latent active site serine to a cysteine (S525C) was isolated and labeled with 5IAF (Flu-II) as described by Brufatto and Nesheim [15]. Phospholipid vesicles composed of 75% PC and 25% PS (PCPS) were prepared as previously described [16]. Bio-Rad Protein Assay reagent was purchased from Bio-Rad (Mississauga, ON, Canada). Corn trypsin inhibitor (CTI) was from Enzyme Research Labs (South Bend, IN, USA). Rivaroxaban and apixaban were purchased from Suzhou Howsine Biological Technology Company (Suzhou, China). Hirudin was purchased from EMD Chemicals, Inc. (Gibbstown, NJ, USA).

Rate of Flu-II cleavage by residual FXa with increasing levels of DOACs – To determine

residual FXa activity upon inhibition by DOACs, Flu-II cleavage was carried out in plasma or whole blood. A mixture (50 µL) containing 0.4 µM Flu-II, 2 µM hirudin, 33 µL of NHP, and either rivaroxaban or apixaban at varying concentrations (0 to 30nM) was monitored continuously with a FlexStation 3 (Molecular Devices, Sunnyvale, CA, USA) fluorescent plate reader at 37ºC at 3-s intervals, with excitation and emission wavelengths at 495 and 540 nm, respectively, with a 530-nm emission cut-off filter. After one minute of equilibration, 50 µL of a mixture containing 0.1 nM FXa, 10 nM FVa, 50 µM PCPS, and 20 mM $CaCl_2$ was added and mixed by instrument trituration. The initial rates of fluorescence change were then measured by determining the slope of the first 15% to 20% of the reaction that is linear, and plotted with respect to the final DOAC concentration in the reaction mixture. To examine whether the assay would be sensitive to individual differences, the DOAC dose-response experiment was repeated using four individual citrated plasma samples without generating a pool.

Next it was tested whether Flu-II cleavage by residual FXa can be measured in whole blood. Rivaroxaban or apixaban was added to citrated whole blood to mimic blood samples collected from patients taking these drugs. A mixture (50 µL) containing 2 µL of whole blood containing varying levels of the DOACs (0 to 100 nM), 0.4 µM Flu-II, and 2 µM hirudin was monitored with FlexStation 3 fluorescent plate reader as described above. Again after one minute of equilibration, 50 µL of a mixture containing 0.1 nM FXa, 10 nM FVa, 50 µM PCPS, and 20 mM $CaCl_2$ was added and mixed by instrument trituration. The initial rates of fluorescence change was then measured and plotted with respect to the final DOAC concentration in the reaction mixture, which results in a 1:50 dilution.

Intra-assay and inter-assay variability – NHP was prepared with known amounts DOACs (2 nM rivaroxaban or apixaban), aliquoted and frozen at –80°C. These samples subsequently were thawed, and each was measured three times on 3 different days using a different standard curve each day. To obtain the intra-assay variability, the standard deviations for each day was determined. The mean of these averages for all 3 days was then determined to be the intra-assay variability. The inter-assay variability was calculated by determining the average of the measurements over 3 days. The average of the standard deviations as percentages of the means was then taken as the inter-assay variability.

Measurement of rivaroxaban or apixaban levels in patient plasma – To ensure that the assay is able to quantify anti-FXa DOAC levels in plasma of patients that are prescribed rivaroxaban or apixaban, random selected samples from the Perioperative Anticoagulant Use for Surgery Evaluation (PAUSE) study were measured for rivaroxaban or apixaban levels [17]. The experiment was performed as described above whereby the known standard in plasma was replaced with the patient plasma to achieve a final dilution of 1:3 in the reaction. To ensure that the measurement levels would be quantifiable within reason, all samples were additionally subjected to a 1:5 dilution to achieve a final dilution of 1:15 in the reaction. Once the DOAC levels were quantified using this assay, the coagulation lab was contacted for the values determined using the chromogenic assay for comparison.

Statistical Analyses – The initial rates of Flu-II cleavage determined in the presence of rivaroxaban or apixaban at varying concentrations were tested for normality and subsequently compared using one-way analysis of variance (SigmaPlot v11, SPSS Inc.). In addition, where applicable, Tukey's post hoc analyses were performed for individual comparisons between groups. P-values <0.05 were considered statistically significant.

Results

Effect of DOAC concentration on the rate of Flu-II cleavage – The initial rates of Flu-II cleavage by prothrombinase in the presence or absence of DOACs at varying concentrations were measured by fluorescence signal change. Using NHP as the background, the initial rate of fluorescence change decreased with increasing levels of DOAC. The initial rates of Flu-II cleavage were dependent on rivaroxaban concentrations between 0 and 5 nM, with the overall inhibition approaching ~85% of total activity (Fig. A1A). The initial rates were also dependent on apixaban concentrations between 0 and 10 nM, with the overall inhibition approaching ~60% (Fig. A1B). The reproducibility of the standard curve is shown in the insets. There were no observable differences in the dose-response curves by the presence of CTI, a commonly used FXIIa inhibitor and anticoagulant [18]. One-way analysis of variance showed significant dose-responses of both rivaroxaban ($p < 0.001$) and apixaban ($p < 0.001$). Post hoc Tukey's test indicated that all rivaroxaban groups were significantly different from each other. For apixaban, all groups were significantly different from each other except for 0 nM *versus* 2 nM ($p = 0.277$) and 2 nM *versus* 5 nM ($p = 0.143$).

Flu-II cleavage in individual plasma samples – Similar trends as those with NHP were observed when the reactions were carried out using plasma samples isolated from different individuals (Fig. A2). Overall trends were similar to those observed with NHP (Fig. A1), whereby rivaroxaban showed greater sensitivity compared with apixaban. In addition, rivaroxaban again demonstrated sensitivity between 0 and 5 nM with the maximal inhibition of ~80% of total FXa activity with great reproducibility between individuals. The assay also showed good reproducibility with apixaban concentrations ranging between 0 and 10 nM, with the maximal inhibition approaching ~50%.

Rate of Flu-II cleavage in whole blood – The initial rate of Flu-II cleavage demonstrated a dose-dependence with concentrations of the DOACs (Fig. A3). Because the reaction results in a 50-fold dilution, the highest dose of the DOAC investigated (2 nM) represents 100 nM circulating in the blood. Unlike with plasma, the dose-response was similar between rivaroxaban and apixaban, with maximal inhibition approaching ~50%. One-way analysis of variance showed significance in the dose-response of both rivaroxaban ($p < 0.001$) and apixaban ($p = 0.007$). Post hoc Tukey's test indicated that all rivaroxaban groups were significantly different between each other except the comparison between 25 nM and 50 nM ($p = 0.136$). For apixaban, only the comparison against the control showed significance.

Determination of the intra-assay and inter-assay variability – To determine the reproducibility of the DOAC assay, the intra-assay variability and inter-assay variability were determined [20]. They were determined by subjecting DOACs at a known concentration (2 nM) in NHP to the current DOAC assay. Each sample was measured four different times on 3 different days using a different standard curve each day. The mean concentration ± SD for four measurements were then calculated. The intra-assay and inter-assay variability for the rivaroxaban assay were determined to be 25.7% and 31.5%, respectively. The intra-assay and inter-assay variability for the apixaban assay were 60.3% and 58.0%, respectively.

Measurement of DOAC levels selected PAUSE study patient samples – To determine whether the assay can be applied to patient samples, we measured patient plasma samples for rivaroxaban and apixaban. Furthermore, to mimic easy point-of-care analyses, the plasma samples were applied directly without any normalization or a singular 10-fold dilution. Of the rivaroxaban samples quantified using our assay, 86% of the samples were deemed unmeasurable using the chromogenic assay (*i.e.* <45 nM or 20 ng/mL). For apixaban containing samples, however, 55% of the samples that we quantified were deemed unmeasurable with the chromogenic assay (Fig. A4). The DOAC levels reported by the chromogenic assay for the samples that were deemed measurable with both assays were 71.4 ± 11.5 nM and 66.9 ± 10.6 nM for rivaroxaban and apixaban, respectively (Table A1).

Discussion

We report a novel assay that is sensitive to levels of DOACs that are well below the current limit of detection at specialized coagulation laboratories (20 ng/mL or 45 nM). Furthermore, the assay utilizes a prothrombin derivative S525C, which is advantageous for a number of reasons. First, because the active site serine is mutated to a cysteine, the resulting thrombin does not possess any proteolytic activity which would otherwise result in a positive feedback and propagation of thrombin generation. To ensure that no endogenous thrombin remains active, a thrombin-specific inhibitor hirudin is added into the assay. Therefore, any prothrombin cleavage observed is as a direct result of FXa that is provided by the assay and not endogenous FXa generated. The second advantage of S525C-prothrombin is labeling of the only free-thiol group on the cysteine with a fluorescent probe such as 5-IAF, so that any fluorescent change observed is simply due to the cleavage of Flu-II by the remaining exogenous FXa. This simplifies the complicated analyses of the entire coagulation cascade, where the initial rate of Flu-II cleavage is simply inversely proportional to DOAC concentrations without needing the resulting thrombin activity to quantify the kinetics of prothrombin activation. The third advantage of using Flu-II is that the assay no longer becomes dependent on the intrinsic coagulation factor composition of the individuals since the output simply depends on the cleavage of Flu-II by the exogenous FXa that is also provided by the assay reagent. This assay is not sensitive to the presence of other coagulation inhibitors such as CTI or vitamin-K antagonists such as warfarin (since all the necessary coagulation factors are provided by the assay and have normally γ-carboxylated GLA domains). The assay is, however,

sensitive to the levels of low-molecular weight heparin (such as dalteparin) and antithrombin in the plasma sample (not shown), whereby dalteparin enhances the inhibitory properties of antithrombin for FXa [19]. The sensitivity to antithrombin could, however, be ameliorated by supplementing the assay with additional antithrombin, whereby physiologic and higher concentrations (2 μM) of antithrombin does not appear to influence the rate of Flu-II cleavage. By doing so, the assay also has the potential to measure low-molecular weight heparin levels in patients.

Because the fluorescence change of Flu-II by FXa is reflective of the activation cleavage at Arg320 of prothrombin to generate the intermediate meizothrombin, the substrate could also be a mutant variant of prothrombin that can only generate meizothrombin as the final product (*e.g.* R271A/Q and/or R155A/Q and/or R284A/Q) to produce similar signal changes [20]. Furthermore, the assay is not necessarily limited to using 5-IAF as the probe to provide a signal change, although the labeling efficiency appears to be better for 5-IAF (~35%) compared with similar probes such as Alexa-488 (~20%).

The range of sensitivity to detect the DOACs can be varied by two methods. The first is to dilute the patient plasma samples containing high DOAC levels using a standard reference DOAC-free plasma so that the residual FXa activity falls within the appropriate range. The second method would be to alter the concentration of the prothrombinase/activating solution; with a higher activator concentration for samples from patients undergoing active therapy or a lower activator concentration for measuring

residual DOAC levels upon cessation of anticoagulation. This flexibility and versatility of the assay allows for tailoring and customization to meet various needs.

While prothrombin activation can be triggered by a number of different reagents such as tissue factor or polyphosphates [21,22], these pathways are more up-stream of where prothrombin activation would take place and thus become dependent on the individual procoagulant potential to activate FX. Therefore, activating the assay system with purified FXa along with FVa, PCPS, and calcium (prothrombinase) makes the assay independent of these individual differences of the up-stream processes needed to generate FXa.

The ability of this assay to measure rivaroxaban or apixaban in whole blood certainly hints at its potential to be used in a point-of-care setting, where a small amount of blood is sufficient to measure the drug levels during active therapy. These methods would be ideal for testing for anticoagulation on an on-going basis to 1) ensure that patients are taking the drugs as recommended to be in therapeutic range, and 2) identify/monitor anticoagulation in patients with altered drug metabolism or clearance (liver or kidney failure, drug-drug interactions or extremes in body weight). This assay as a point-of-care strategy would certainly provide the means for personalized treatment and care during anticoagulation.

Clinical trials are under way to investigate how measurable levels of DOACs at the time of surgical intervention are correlated with bleeding complications [17]. Since readily available methods of measurements cannot detect below 20 ng/mL, this assay can be implemented into such study comparing residual anti-FXa DOAC levels with bleeding

complications, specifically investigating whether bleeding can be correlated with DOAC levels below the current detection limit of clinically used assays.

Disclosure of Conflict of Interests

P.L.G. has received honoraria from Bayer, Bristol Myers Squibb, Pfizer, Leo Pharma, and Servier. J.D.D. has received honoraria from AstraZeneca, Bayer, Biotie, Boehringer-Ingelheim, Bristol Myers Squibb, Daiichi Sankyo, Pfizer, Portola, Sanofi, and The Medicines Company. The other authors have no conflict of interest.

Acknowledgements

P.Y.K. is supported by the Hamilton Health Sciences Early Career Award and the New Investigator Fund. L.R.D is supported by The Canadian Venous Thromboembolism Clinical Trials and Outcomes Research (CanVECTOR) Network Studentship Award. This work was also supported by the Division of Hematology & Thromboembolism (McMaster University) and CanVECTOR Network Research Grant. We thank Dr. James C. Fredenburgh for critically reviewing the manuscript.

Author Contribution: P.Y.K. conceptualized and designed experiments, and wrote the manuscript. P.L.G. designed experiments and wrote the manuscript. C.W. performed experiments to develop the assay (Figs A1 through A3). L.R.D. performed the assay on clinical samples (Fig A4) and edited the manuscript. J.D.D. provided the PAUSE study samples along with their measured properties, and edited the manuscript.

References

1. ten Cate H. New oral anticoagulants: discussion on monitoring and adherence should start now! *Thromb J* 2013; **11:** 8.

2. Salmela B, Joutsi-Korhonen L, Armstrong E, Lassila R. Active online assessment of patients using new oral anticoagulants: bleeding risk, compliance, and coagulation analysis. *Semin Thromb Hemost* 2012; **38:** 23-30.

3. Mismetti P, Laporte S. New oral antithrombotics: a need for laboratory monitoring. For. *J Thromb Haemost* 2010; **8:** 621-6.

4. Spyropoulos AC, Douketis JD. How I treat anticoagulated patients undergoing an elective procedure or surgery. *Blood* 2012; **120:** 2954-62.

5. Tran H, Joseph J, Young L, McRae S, Curnow J, Nandurkar H, Wood P, McLintock C. New oral anticoagulants: a practical guide on prescription, laboratory testing and peri-procedural/bleeding management. Australasian Society of Thrombosis and Haemostasis. *Intern Med J* 2014; **44:** 525-36.

6. Gladstone DJ, Geerts WH, Douketis J, Ivers N, Healey JS, Leblanc K. How to Monitor Patients Receiving Direct Oral Anticoagulants for Stroke Prevention in Atrial Fibrillation: A Practice Tool Endorsed by Thrombosis Canada, the Canadian Stroke Consortium, the Canadian Cardiovascular Pharmacists Network, and the Canadian Cardiovascular Society. *Ann Intern Med* 2015; **163:** 382-5.

7. Narouze S, Benzon HT, Provenzano DA, Buvanendran A, De Andres J, Deer TR, Rauck R, Huntoon MA. Interventional spine and pain procedures in patients on antiplatelet and anticoagulant medications: guidelines from the American Society of Regional Anesthesia and Pain Medicine, the European Society of Regional Anaesthesia and Pain Therapy, the American Academy of Pain Medicine, the International Neuromodulation Society, the North American Neuromodulation Society, and the World Institute of Pain. *Reg Anesth Pain Med* 2015; **40:** 182-212.

8. Douketis JD, Syed S, Schulman S. Periprocedural Management of Direct Oral Anticoagulants: Comment on the 2015 American Society of Regional Anesthesia and Pain Medicine Guidelines. *Reg Anesth Pain Med* 2016; **41:** 127-9.

9. Samuelson BT, Cuker A, Siegal DM, Crowther M, Garcia DA. Laboratory Assessment of the Anticoagulant Activity of Direct Oral Anticoagulants: A Systematic Review. *Chest* 2017; **151:** 127-38.

10. Schlitt A, Jambor C, Spannagl M, Gogarten W, Schilling T, Zwissler B. The perioperative management of treatment with anticoagulants and platelet aggregation inhibitors. *Dtsch Arztebl Int* 2013; **110:** 525-32.

11. Cuker A, Siegal DM, Crowther MA, Garcia DA. Laboratory measurement of the anticoagulant activity of the non-vitamin K oral anticoagulants. *J Am Coll Cardiol* 2014; **64:** 1128-39.

12. Samama MM, Contant G, Spiro TE, Perzborn E, Guinet C, Gourmelin Y, Le Flem L, Rohde G, Martinoli JL. Evaluation of the anti-factor Xa chromogenic assay for the measurement of rivaroxaban plasma concentrations using calibrators and controls. *Thromb Haemost* 2012; **107:** 379-87.

13. Stangier J, Rathgen K, Stahle H, Gansser D, Roth W. The pharmacokinetics, pharmacodynamics and tolerability of dabigatran etexilate, a new oral direct thrombin inhibitor, in healthy male subjects. *Br J Clin Pharmacol* 2007; **64:** 292-303.

14. Samama MM, Contant G, Spiro TE, Perzborn E, Le Flem L, Guinet C, Gourmelin Y, Rohde G, Martinoli JL. Laboratory assessment of rivaroxaban: a review. *Thromb J* 2013; **11:** 11.

15. Brufatto N, Nesheim ME. The use of prothrombin(S525C) labeled with fluorescein to directly study the inhibition of prothrombinase by antithrombin during prothrombin activation. *J Biol Chem* 2001; **276:** 17663-71.

16. Bloom JW, Nesheim ME, Mann KG. Phospholipid-binding properties of bovine factor V and factor Va. *Biochemistry* 1979; **18:** 4419-25.

17. Douketis JD, Spyropoulos AC, Anderson JM, Arnold DM, Bates SM, Blostein M, Carrier M, Caprini JA, Clark NP, Coppens M, Dentali F, Duncan J, Gross PL, Kassis J, Kowalski S, Lee AY, Le Gal G, Le Templier G, Li N, MacKay E et al. The Perioperative Anticoagulant Use for Surgery Evaluation (PAUSE) Study for Patients on a Direct Oral Anticoagulant Who Need an Elective Surgery or Procedure: Design and Rationale. *Thromb Haemost* 2017; **117:** 2415-24.

18. Swartz MJ, Mitchell HL, Cox DJ, Reeck GR. Isolation and characterization of trypsin inhibitor from opaque-2 corn seeds. *J Biol Chem* 1977; **252:** 8105-7.

19. Hirsh J, Anand SS, Halperin JL, Fuster V. Mechanism of action and pharmacology of unfractionated heparin. *Arterioscler Throm Vasc Biol* 2001; **21:** 1094-6.

20. Kim PY, Yeh CH, Dale BJ, Leslie BA, Stafford AR, Fredenburgh JC, Hirsh J, Weitz JI. Mechanistic basis for the differential effects of rivaroxaban and apixaban on global tests of coagulation. *Thrombosis & Haemostasis Open* 2018; **2:** e190-e201.

21. Gajsiewicz JM, Morrissey JH. Structure-Function Relationship of the Interaction between Tissue Factor and Factor VIIa. *Semin Thromb Hemost* 2015; **41:** 682-90.

22. Smith SA, Mutch NJ, Baskar D, Rohloff P, Docampo R, Morrissey JH. Polyphosphate modulates blood coagulation and fibrinolysis. *Proc Natl Acad Sci U S A* 2006; **103:** 903-8.

Table A1. Comparison of the DOAC values for each sample that was able to be measured by both Flu-II and chromogenic assays.

DOAC	Sample ID	Flu-II Assay (nM)	Chromogenic (nM)
Rivaroxaban	Sample 2333	3.6	83.3
	Sample 1456	7.6	58.5
	Sample 3420	7.6	78.8
	Sample 1423	4.0	65.3
	Average	5.7 ± 2.2	71.4 ± 11.5
Apixaban	Patient 3152	1.7	56.3
	Patient 3190	7.9	47.3
	Patient 3193	2.2	78.8
	Patient 1425	5.8	72.0
	Patient 3147	2.1	65.3
	Patient 3248	6.2	60.8
	Patient 2914	1.7	81.0
	Patient 3266	6.6	58.5
	Patient 3155	5.1	67.5
	Patient 3261	2.0	78.8
	Patient 3169	19.6	63.0
	Average	8.3 ± 5.2	66.9 ± 10.6

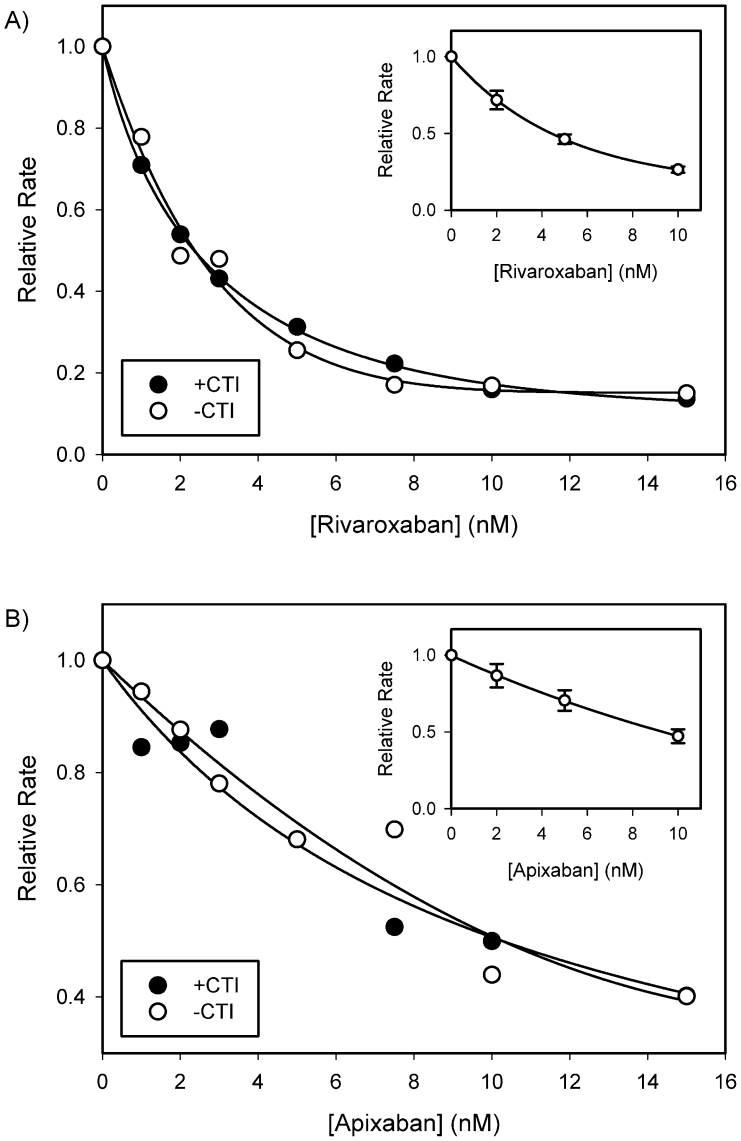

Figure A1. Residual FXa activity as a function of increasing concentration of A) rivaroxaban, or B) apixaban, with (*closed*) or without (*open*) CTI. To determine residual FXa activity upon inhibition by DOACs, Flu-II cleavage was carried out in plasma. A mixture (50 µL) containing 0.4 µM Flu-II, 2 µM hirudin, 33 µL of NHP, and either rivaroxaban or apixaban at varying concentrations (0 to 30nM) was placed in a clear-bottom 96-well microtiter plate. Fluorescence was monitored using excitation and emission wavelengths at 495 and 540 nm, respectively, with a 530-nm emission cut-off filter. After one minute of equilibration, 50 µL of a mixture containing 0.1 nM FXa, 10 nM FVa, 50 µM PCPS, and 20 mM $CaCl_2$ was added and mixed by FlexStation 3 instrument trituration. The initial rates of fluorescence change was then measured and plotted with respect to the final DOAC concentration in the reaction mixture, which results in a 1:2 dilution. *Inset* shows the reproducibility of the standard curves generated in the absence of CTI (n = 6).

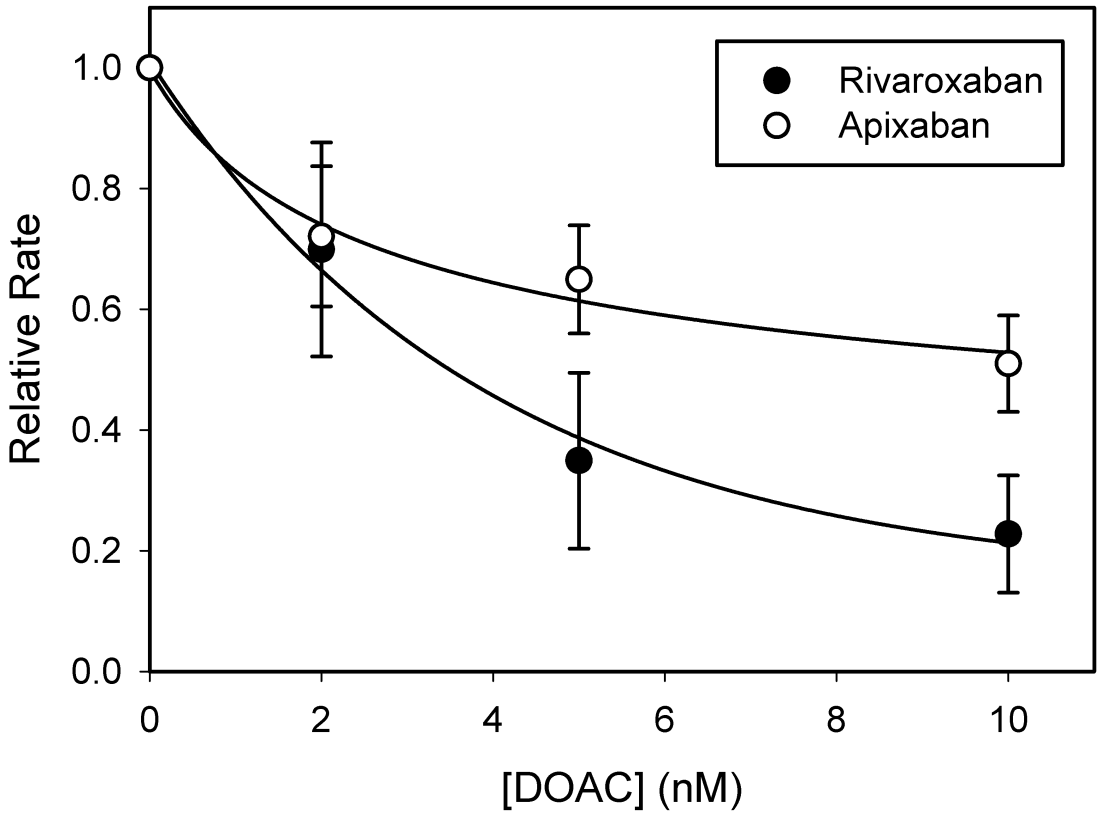

Figure A2. Dose response of the assay to anti-FXa-DOACs in individual plasma samples. Four different individuals were tested with the assay. Either rivaroxaban (*closed*) or apixaban (*open*) was added into the isolated plasma samples to a final concentration ranging between 0 and 10 nM. The rates were normalized to no DOACs added. Symbols indicate mean ± SD (n = 4).

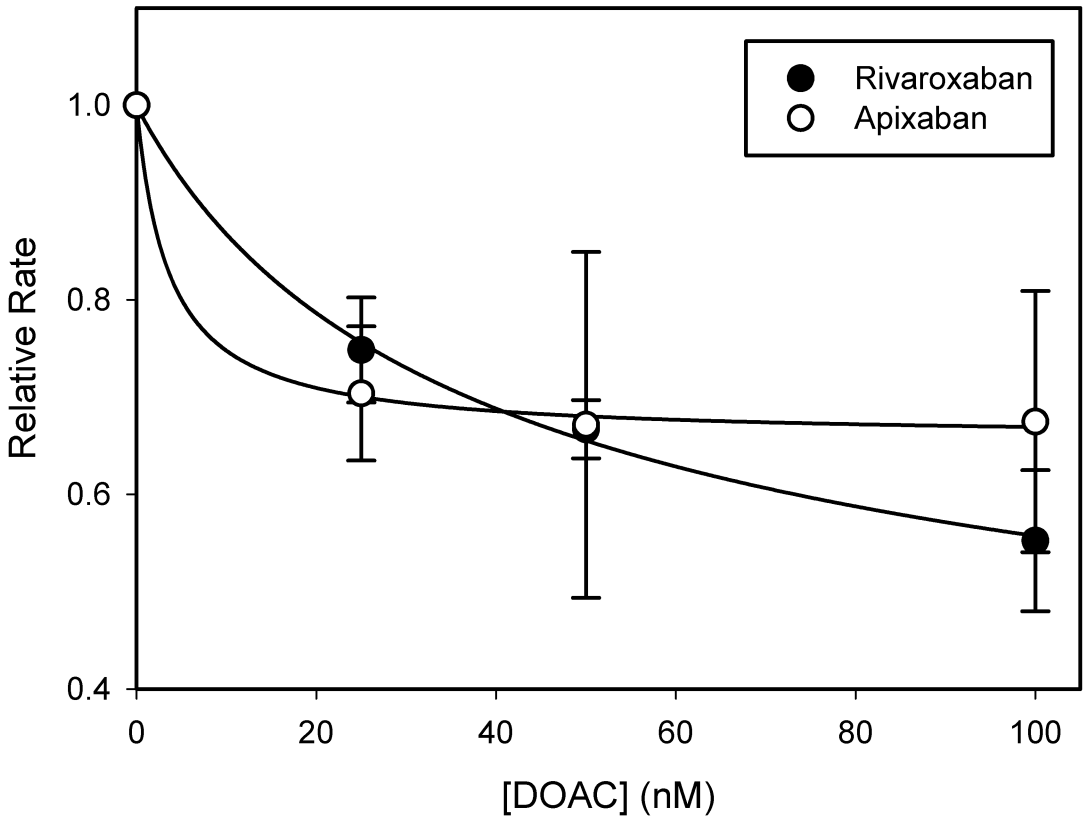

Figure A3. Dose response of the assay to anti-FXa-DOACs in whole blood. Whole blood was collected in citrate to which rivaroxaban (*closed*) or apixaban (*open*) was added to achieve an in-blood concentration ranging between 0 and 100 nM. Similar to above, a mixture (50 µL) containing 0.4 µM Flu-II, 2 µM hirudin, 2 µL of whole blood containing rivaroxaban or apixaban was placed in a clear-bottom 96-well microtiter plate. Fluorescence was monitored using excitation and emission wavelengths at 495 and 540 nm, respectively, with a 530 nm emission cut-off filter. After one minute of equilibration, 50 µL of a mixture containing 0.1 nM FXa, 10 nM FVa, 50 µM PCPS, and 20 mM $CaCl_2$ was added and mixed by FlexStation 3 instrument trituration. The initial rates of fluorescence change was then measured and plotted with respect to the final DOAC concentration in the reaction mixture, which results in a 1:50 dilution. (n >= 3)

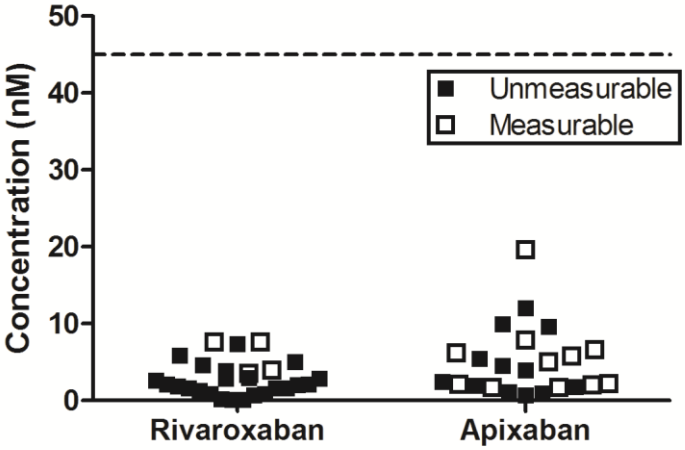

Figure A4. Quantification of the PAUSE study patient plasma samples containing rivaroxaban or apixaban. Random patient samples were quantified using the generated standard curve. Majority of the samples that were quantifiable with the Flu-II assay were deemed unmeasurable using the chromogenic assay (*closed*) while the remainder were measurable with both assays (*open*). The values of the samples that were quantified by both assays are shown in Table A1. The dotted line represents the detection limit of the chromogenic FXa activity assay.